A boundary vector cell model of place field repetition

Roddy M. Grieves[1], Éléonore Duvelle[1], Paul A. Dudchenko[2,3]

[1]University College London
Institute of Behavioural Neuroscience
Department of Experimental Psychology
London,
United Kingdom

[2]School of Natural Sciences,
University of Stirling,
Stirling,
United Kingdom

[3]Centre for Cognitive and Neural Systems,
Edinburgh Medical School: Biomedical Sciences,
University of Edinburgh,
Edinburgh,
United Kingdom

Key words: place cell; boundary vector cell; computational model; border cell, field repetition; fragmentation; multicompartment

14 figures

Accepted for publication in *Spatial Cognition and Computation* published by Taylor and Francis

Abstract

Hippocampal place cells are thought to form the neural substrate of a global cognitive map. However, in multicompartment mazes these cells exhibit locally repeating representations, undermining the global cognitive map view of place cells. This phenomenon appears to be related to the repetitive layout of these mazes, but still no hypothesis adequately explains it. Here, we use a boundary vector cell model of place cell firing to model the activity of place cells in numerous multicompartment environments. The activity of modelled place cells bears a striking resemblance to experimental data, replicating virtually every major experimental result. Our results support the boundary vector cell model and indicate that locally repeating place cell firing could result purely from local geometry.

Introduction

Place cells

Place cells are neurons in the hippocampus that increase their firing rate when an animal visits specific regions of its environment (O'Keefe, 1979; O'Keefe & Conway, 1978; O'Keefe & Nadel, 1978). Different place cells have 'place fields' in different areas of an environment, so that together the entire surface of an environment is represented (O'Keefe, 1976; Wilson & McNaughton, 1993). The main argument of the current work is that place fields are driven by local geometric features, for example the walls of a maze. To test this, we used a computational model based on inputs to place cells from cells that encode the distance and direction of local boundaries.

Several properties of place cells make them an ideal neural substrate for spatial navigation (O'Keefe & Nadel, 1978) and memory (Eichenbaum et al., 1999). For example, once a place field has formed, it is stable across days (Muller, Kubie, & Ranck, 1987) and even weeks (Thompson & Best, 1990). If an environment is altered or completely novel, place cells may change their firing relationship, forming a representation seemingly unique to this space (O'Keefe & Conway, 1978; Alme et al., 2014), a process known as 'remapping' (Anderson & Jeffery, 2003; Leutgeb et al., 2005; Muller & Kubie, 1987). Remapping can be induced by changing the geometry of an environment (Muller & Kubie, 1987), or by changing the color of a visual cue (Bostock et al, 1991) or an environment's walls (Kentros et al, 2004; Anderson & Jeffery, 2003). Hippocampal activity can be used to decode the current position of an animal in real-time (Pfeiffer & Foster, 2013) and has been implicated in the planning of future trajectories (Bendor & Spiers, 2016; Grieves et al. 2016a; Pfeiffer & Foster, 2013). Similar activity is also apparent during sleep, where it is thought to underlie memory consolidation (Girardeau et al. 2009). As we will consider below, however, there are properties of place fields that are inconsistent with a global spatial representation.

Place field repetition

Place cells, when recorded in multicompartment and multialleyway environments, express multiple firing fields in similar locations within each sub-compartment. For instance, Skaggs and McNaughton (2005), Fuhs et al. (2005) and Tanila (1999) all demonstrated that, in two identical compartments connected by a corridor or a doorway, many place cells represent the two compartments more similarly than would be expected by chance (Figure 1). Similarly, Spiers et al. (2015), Grieves et al. (2016b) and Harland et al. (2017) extended this apparatus to four compartments and observed repeating place fields (Figure 1). Carpenter et al. (2015) reported the same phenomenon in grid cells and Derdikman et al. (2009) reported that both grid and place cells simultaneously exhibit repeating fields in up to five parallel alleyways with the same orientation. Frank et al. (2000) and Singer et al. (2010) found similar results in multialleyway mazes. For a review of the literature surrounding this phenomenon, see Grieves et al. (2017).

The spatial map formed from these repeating, local representations is unlikely to be optimal for non-local spatial navigation. Indeed, computational analysis suggests that repeating place fields provide poor information for decoding an animal's position (Spiers et al. 2015) and experimental evidence suggests they are accompanied by spatial learning deficits (Grieves et al., 2016b). Why place cells form these repeating representations is largely unknown. While field repetition is likely linked to the repetitive design of these environments, it does not seem to result from identical visual inputs because both Derdikman et al. (2009) and Grieves et al. (2016b) observed repeating fields despite providing distal cues that should have polarised at least some compartments or alleyways. Repeating fields can also be observed in environments

without illumination (Grieves, 2015). Likewise, repeating place fields cannot be due to place cells encoding body movements or response sequences in a stereotyped task because they can be observed in environments where animals are free to explore and behave naturally (Grieves et al., 2016b; Spiers et al., 2015). Moreover, this phenomenon does not seem to be purely due to disorientation in vastly ambiguous environments since place field repetition can be seen in as little as two (Fuhs et al., 2005; Skaggs & McNaughton, 1998; Tanila, 1999) and as many as five (Derdikman et al., 2009) compartments. Yet, a common feature in each of these experiments is repetitive local compartments. Thus we hypothesise that geometry must play a fundamental role in the repetition of place fields.

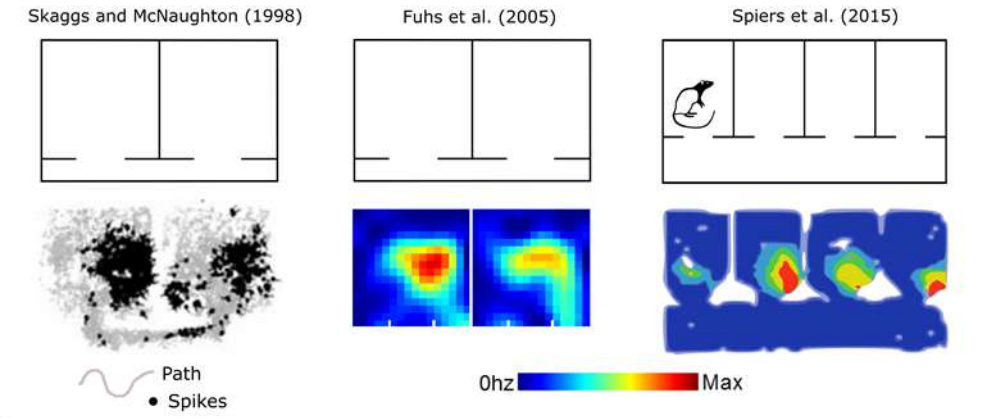

Figure 1 Mazes where repeating place field patterns have been observed. ***Top row***; floor plan maze diagrams. ***Bottom row***: the response of a single neuron either showing the path of the animal and the position of the cell's action potentials or a firing rate map of the cell's activity.

BVCs and boundary cells

To initialise and maintain a consistent spatial map, place cells appear to rely on distal cues or landmarks surrounding an environment. If these landmarks are rotated, the firing fields of place cells rotate correspondingly (Muller & Kubie, 1987; O'Keefe & Conway, 1978; Yoganarasimha & Knierim, 2005). However, place cell firing also appears to be influenced by

the geometry of an environment. For instance, when elongating a square environment into a rectangle, previously small and round place fields can be seen to stretch in proportion to the walls, becoming long and distended (O'Keefe & Burgess, 1996) and place cells recorded in differently shaped, but resembling environments often appear to have place fields in similar locations (Lever, Wills, Cacucci, Burgess, & O'Keefe, 2002). These geometric determinants led researchers to formulate a model of place cell firing which employed hypothetical Boundary Vector Cells (BVCs). BVCs fire in relation to environmental boundaries at a specific distance and direction from an animal (Figure 2). The sensitivity of these cells is controlled by distal cues (i.e., visual cues that are not directly accessible by the animal) and place cell firing has been proposed to arise from the thresholded sum activity of a subpopulation of BVCs (Barry et al., 2006; Burgess, Donnett, Jeffery, & O'Keefe, 1997; Burgess, Jackson, Hartley, & O'Keefe, 2000; Hartley, Burgess, Lever, Cacucci, & O'Keefe, 2000; Lever, Burgess, Cacucci, Hartley, & O'Keefe, 2002)(Figure 3). This model explains very well the geometric features of place cell firing.

Following the introduction of the BVC model, neurons similar to BVCs have been observed in a number of brain regions including the subiculum (Barry et al., 2006; Lever, Burton, Jeewajee, O'Keefe, & Burgess, 2009; Sharp, 1999; Stewart, Jeewajee, Wills, Burgess, & Lever, 2014), parasubiculum (Boccara et al., 2010; Solstad, Boccara, Kropff, Moser, & Moser, 2008), medial entorhinal cortex (mEC)(Bjerknes, Moser, & Moser, 2014; Savelli, Yoganarasimha, & Knierim, 2008; Solstad et al. 2008) and recently the rostral thalamus (Jankowski et al., 2015) and anterior claustrum (Jankowski & O'Mara, 2015) (Figure 2). These 'boundary' cells have a preferred firing direction, much like head direction cells, but instead of firing maximally when the animal's head is facing this direction, a given boundary cell will fire when an environmental boundary lies in that direction from the animal. This firing is driven by the boundary's position relative to the animal, presumably based on self-motion information.

Consistent firing is observed in every environment where the cell is recorded, provided that the external reference frame is maintained. For instance, consistent boundary fields are anticipated if each environment is placed in the same curtain enclosure with the same distal cue card (Lever et al., 2009; Sharp, 1997). Environmental boundaries which can drive cell firing in this way may be walls, low ridges or vertical drops and the colour, texture or odour of these does not seem to influence the cell's firing (Lever et al., 2009).

The proposition that place cell firing may be the result of boundary cell input as opposed to other cell types such as grid cells has gained recent support (Barry & Burgess, 2007; Bush, Barry, & Burgess, 2014; Hartley, Burgess, Lever, Cacucci, & O'Keefe, 2000). At 2.5 weeks of age, rat pups already have an internal representation of their environment in the form of relatively stable place fields capable of remapping (Muessig et al. 2016) and a fully functional head direction signal. However, their grid cells have still not fully developed a hexagonal grid firing pattern (Bjerknes, Moser, & Moser, 2014; Langston et al., 2010) and do not exhibit them until 3 weeks of age (Wills, Barry, & Cacucci, 2012). In contrast, before 2.5 weeks of age boundary cells in the mEC are already fully developed (Bjerknes et al., 2014) and place cell activity is significantly more stable near to environmental boundaries (Muessig et al. 2015). These findings, in conjunction with the accuracy with which BVC models can account for and even predict place cell firing in multiple environments suggests that boundary cells play a role in the development, formation and maintenance of hippocampal spatial representations.

If geometry plays a role in the repetition of place fields, utilising a purely geometric model of place cell activity based on BVCs should explain why we observe repetition in multicompartment and multialleyway environments. By their very definition, boundary cells are sensitive to environmental geometry and a model in which place cell firing is at least partially dictated by their inputs should also predict the pattern of results observed in the multicompartment environments described above. Thus, we predict that if place field repetition is purely the result of local geometry then we should be able to accurately model the activity of

place cells in each of the environments described above using only geometric inputs. If this is the case it would indicate that place cells preferentially utilise local, geometric information which is then stitched together to form a larger 'map' of an environment. This would undermine the view that the hippocampus forms a unified global cognitive map of complex environments – at least initially - because it suggests large scale spatial representations in the brain are actually composed of small scale geometric ones. If the model is inaccurate, however, this would suggest that repetitive local geometries are not sufficient to drive place field repetition.

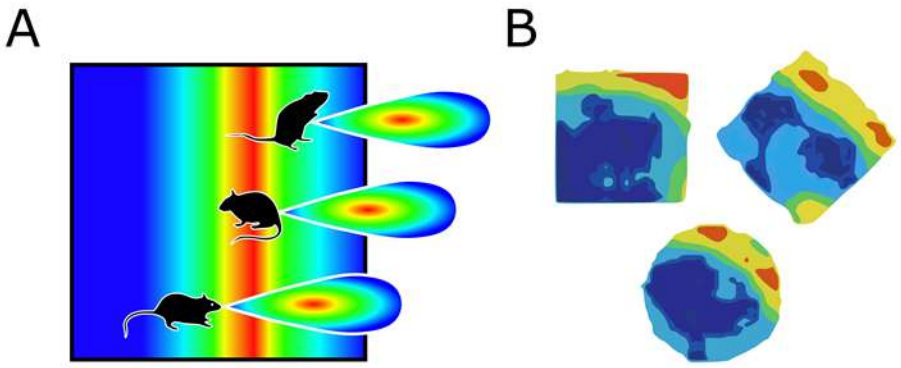

Figure 2 Implementation of the boundary vector cell model. ***A,*** figure adapted from Barry et al. (2006) describing the overlapping Gaussians contributing to the firing of a BVC sensitive to boundaries found an angle of 0° to the rat and at a distance of 30cm. The right boundary of this environment satisfies the directional component of the BVC. As the rat moves towards and away from it, firing increases and decreases depending on its preferred firing distance. ***B,*** firing rate maps for a single boundary cell recorded in the subiculum in a square, diamond and circular environment (adapted from Lever et al. (2009), figure 3, cell 2d).

Overall Methods

The BVC model

As in Hartley et al. (2000) and Barry et al. (2006), the spatially receptive bounds of our BVCs were modelled as the product of two Gaussians. One varies as a function of the rat's distance from a boundary, the other varies as a function of the angle this boundary presents at the rat. To implement this, we created scale models of the environments reported in the literature and partitioned these into pixels such that each pixel was equivalent to 1 cm square. Then, for every pixel in the environment, for every direction in the range (0, 2π], we calculated the distance (*r*) from the pixel to the nearest boundary segment at that direction (*θ*) and the angle (Δ) that segment subtended to the pixel. Thus, for a given BVC_i that is optimally responsive to boundaries at a distance d_i and at an angle α_i relative to the rat, the receptive field would be described by:

$$f_i(r,\theta,\Delta) \propto \frac{\exp\left(-\frac{(r-d_i)^2}{2\sigma_{rad}^2(d_i)}\right)}{\sqrt{2\pi\sigma_{rad}^2(d_i)}} \times \frac{\exp\left(-\frac{(\theta-\alpha_i)^2}{2\sigma_{ang}^2}\right)}{\sqrt{2\pi\sigma_{ang}^2}} \times \Delta$$

To generate an overall map of the cell's activity for an environment the above equation is applied to every pixel, for all directions in the range (0, 2π] and each pixel's overall value is the linear sum of these results. In this way, all boundaries visible by direct line of sight contribute to the firing of the cell at any given position.

Parameter σ_{ang} is a constant which describes the extent of the cell's angular tuning width and σ_{rad} is a variable parameter which describes the cell's sensitivity to boundaries in terms of distance. This varies in a linear way with distance such that cells with a larger preferred firing distance have wider firing fields. This linear increase is described by:

$$\sigma_{rad}(d_i) = (d_i / \beta + 1)\sigma_0$$

where β and σ_0 represent constants which determine the rate at which the field increases in size with distance and the radial width of the field at a distance of 0 cm, respectively.

Generating place cells

As in Hartley et al. (2000), we modelled the activity of place cells as the combined input of 2 or more BVCs. However, rather than generating place cells as the linear sum of *n* BVCs, as is the case in previous BVC models, we chose to calculate the geometric mean (Figure 3). This consists of taking the *n*th root of the product of *n* BVCs and is given by:

$$F(x) \;=\; u((\prod_{i=1}^{n} f_i(x) \,/\, max_x)^{\frac{1}{n}}) - T$$

where *F* is a place cell, f_i is a BVC, *x* is a location in the rate map of the cell, *T* is the cell's threshold and *u* represents a Heaviside step function ($u(x) = x$, if $x > 0$, otherwise $u(x) = 0$) (Barry et al., 2006). In this way, *T* and *u* act together as a linear threshold on the cell's output. Calculating the product of BVCs results in much better spatial tuning of the resulting place cell and accurately captures much of the features seen in vivo, especially in tight alleyway mazes which compose half of the environments modelled here. Multiplicative neural processes have been reported previously (Peña & Konishi, 2001; 2004), thus it is possible that boundary cell inputs act multiplicatively on postsynaptic place cells (Schnupp & King, 2001), although evidence for this has not yet been shown. One problem is that, as the number of BVCs increases, the resulting place cell activity decreases as a power function of the inputs. The geometric mean therefore acts to normalise the result of this product and was used primarily for this purpose - we note that linear summation and multiplication alone produce similar results to those reported here (data not shown). As a further step we also multiplied *F(x)* by 500 in order to scale the majority of PC spatial maps so that their maximum fell between 1 and 20Hz which are generally accepted cutoffs for place cells (Grieves et al., 2016b). However, a different coefficient could be used to better model the proportion of active and silent cells in a given

environment (Thompson & Best, 1989). Note also that BVCs are normalised between 0 and 1 (by division of their maximum, max_x), meaning that each BVC contributes equally to the firing of

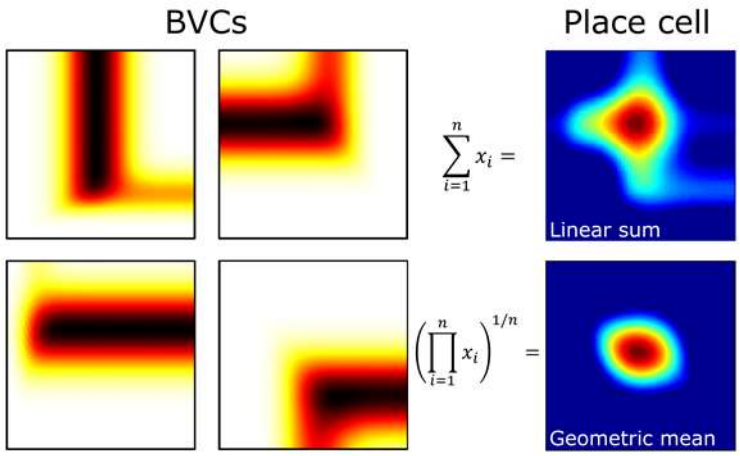

Figure 3 A geometric mean approach to combining BVC inputs. ***Left,*** activity of four modelled BVCs in a 128cm square. ***Top right****,* result combining BVC information by linearly summing across all four BVC ratemaps. ***Bottom right***, geometric mean result. Both place cell maps have been produced using the same final threshold (30% of the maximum), however, the geometric mean approach yields a more spatially tuned response.

a place cell.

In another departure from earlier implementations of the BVC model, instead of drawing BVC preferred distances from a discrete distribution (Hartley et al., 2000) we selected distances from a continuous Gaussian constrained between 6 and 256 cm (μ = 0 cm, σ = 100 cm). This largely biases the population of BVCs towards shorter preferred firing distances which better represent the population of BVCs found in the subiculum (Lever et al., 2009) and border cells in the mEC (Savelli, Yoganarasimha, & Knierim, 2008; Solstad et al., 2008). Preferred firing angles were selected randomly from the uniform distribution (0, 2π]. Each place cell was modelled as the geometric mean of *n* BVCs where *n* was drawn from a Poisson distribution constrained between 2 and 16 (λ = 4 cells). We reasoned that the brain generates place cells using as few

connections and computations as possible and, in reality, this distribution does not often exceed 10 inputs. However, we note that varying the number of inputs of our geometric mean model does not change the overall results and place cells can be generated reliably using 2 to 24 BVCs. It may be desirable to select BVCs non-randomly based on their preferred firing direction, to prevent generating place cells using 2 BVCs with very similar firing patterns. We did not implement this constraint for computational simplicity and because this is not an obvious biological trait of the subicular inputs to the hippocampus.

We modelled the activity of place cells and BVCs in several environments, some of which were open-field control environments where we sought to demonstrate the functionality of the model, such as square (64 x 64cm and 128 x 128cm) and rectangular (64 x 128cm and 128 x 64cm) environments similar in size to those used by Lever et al. (2009) and O'Keefe and Burgess (1996). We also used circular environments (64cm and 128cm in diameter) similar in size to those used by Muller and Kubie (1987) or to a watermaze (Morris, 1981) respectively. We also modelled a 64cm square environment with a wall extending halfway across its central diameter which has been used previously to demonstrate place field repetition (Barry et al., 2006; Lever, Cacucci, Burgess & O'Keefe, 1999).

Additionally, we modelled mazes in which researchers have previously shown place field repetition. These mazes were the two compartment mazes used by Skaggs and McNaughton (1998), Fuhs et al. (2005) and Tanila (1999), the 'hairpin' maze used by Derdikman et al. (2009), the square and circular spiral tracks used by Nitz et al. (2011) and Cowen and Nitz (2014), the four compartment mazes used by Spiers et al. (2015), the two configurations used by Grieves et al. (2016b) and a multi-alleyway maze similar to that used by Frank et al. (2000), Singer et al. (2010) and Grieves (2015).

For the purposes of this study we generated 10,000 BVCs in each of these environments such that a spatial map was produced for each BVC in every environment. The preferred firing distances and directions were maintained for these BVCs across environments,

thus, a change in a given BVC's spatial activity between environments is due to changes in the structure of the environment rather than a change in the cell's characteristics. We then generated 1,500 place cells in all environments. Each place cell received consistent BVC inputs across all environments, and thus differences in place cell firing were due to changes in underlying BVC activity rather than changes in BVC connectivity.

Place field analyses

Unless otherwise stated, all analyses were performed on the unsmoothed firing rate maps produced using the above method, generated at a pixel resolution where 1 pixel = 1 cm^2. When detecting place fields, we looked for areas of more than 9 contiguous pixels with a firing rate greater than 20% of the maximum value in the ratemap. The area, position (taken as the weighted centroid), dimensions and firing rate properties of these fields were then extracted and their ellipticity calculated. Ellipticity was defined as the ratio between the major and minor axis lengths:

$$\varepsilon = \frac{\alpha - \beta}{\alpha} = 1 - \frac{\beta}{\alpha}$$

where α represents the length of the semi-major axis and β represents the length of the semi-minor axis' length. This gives a measure of the curvature of the place field, such that an ellipticity of 0 would represent a circle and an ellipticity of 1 would represent a straight line (although these are degenerate cases).

Morphing

For morphing analyses we used an algorithm described previously (Lever et al., 2002). Briefly, we found the correspondence such that each point maintains its radial position as a proportion of the distance to the perimeter along that radius. For instance, if we wish to morph map 1 (m_1) into the shape of map 2 (m_2) we can achieve this using an inverse lookup transformation whereby we fill each pixel of map 2 using the closest pixel in map 1. For our

method we defined the closest pixel as the one with the same angle from the centre of the map (θ) and the same ratio of distance from the centre to the edge (r). From this it follows that for all points in m_2:

$$m_2(r, \theta) = m_1(r, \theta)$$

See figure 4A for a schematic of this procedure.

Open field environments

A geometric model of place cell firing carries a number of basic predictions that we sought to verify in our own modelled place cell data. For instance, one prediction of the BVC model is that place cells should exhibit similar representations for environments of different shapes (Hartley et al., 2000; O'Keefe & Burgess, 1996). Lever et al. (2002) demonstrated this effect by showing that place cells in square and circular environments containing the same visual cue had very similar firing rate maps (at least initially), when the rate map of one environment was 'morphed' into the shape of the other. O'Keefe and Burgess (1996) similarly demonstrated that place cells recorded in a square environment often exhibit distended or elongated firing fields when the environment was stretched along one dimension and suggested that this response could be explained in terms of a boundary interaction on place cell firing. Conversely, if instead of being stretched an environment is bisected in half by a barrier, place cells will often fire similarly in the spaces on either side of it (Barry et al., 2006), provided that those spaces share a similar local geometry (Paz-Villagrán, Save, & Poucet, 2004).

Methods for open fields

We modelled the activity of place cells in a small square, diamond and circular environment (all 64cm in length or diameter) and in a large square and circular environment (both 128cm in length or diameter). For each place cell we then morphed the activity in each environment into the shape of every other environment using the method described above. We

then correlated these maps to determine how similarly cells represent environments of different shapes and sizes. We also compared the median place field area and ellipticity of these cells in a small square, large square and two rectangles elongated along each dimension as reported by O'Keefe & Burgess (1996). Finally, we modelled the activity of cells in a 64cm square bisected by a 32cm barrier and calculated the level of correlation between the two halves of the environment divided along this barrier. We compared this distribution to one calculated using the same method on a square environment with no barrier.

Results for open fields

Place fields do not expand in proportion to the environment, and similarly sized environments are represented similarly

In the diamond, small square, large square, small circle and large circle environments we observe a similar proportion of active (firing > 1Hz) cells (1209 or 19.4%, 1212 or 19.2%, 1207 or 19.5%, 1178 or 21.5%, 1106 or 26.3% respectively; $z = 15$, $p > .05$, Wilcoxon signed rank test) and cells exhibit a similar number of place fields in each environment (Md = 1 in all cases). However, we find that place fields do not expand in direct relation to the size of the environment. For instance, the mean ratio between field area in the small and large square environment is 1.8, not 4 as would be expected based on the surface area of the environments and between the circular mazes it is 1.9 (expected would be 4). When comparing the morphed spatial firing maps for these environments, they are all more similar than would be expected by chance ($p < .0001$ and $r > 0.3$ in all cases, Wilcoxon rank sum tests (WRSt)). However, morphed versions of similarly sized environments are consistently more similar than those of different sized environments ($z = 54.9$, $p < .0001$, $r = 0.45$, WRSt, Md = 0.69 and 0.30 respectively) (Figure 4A).

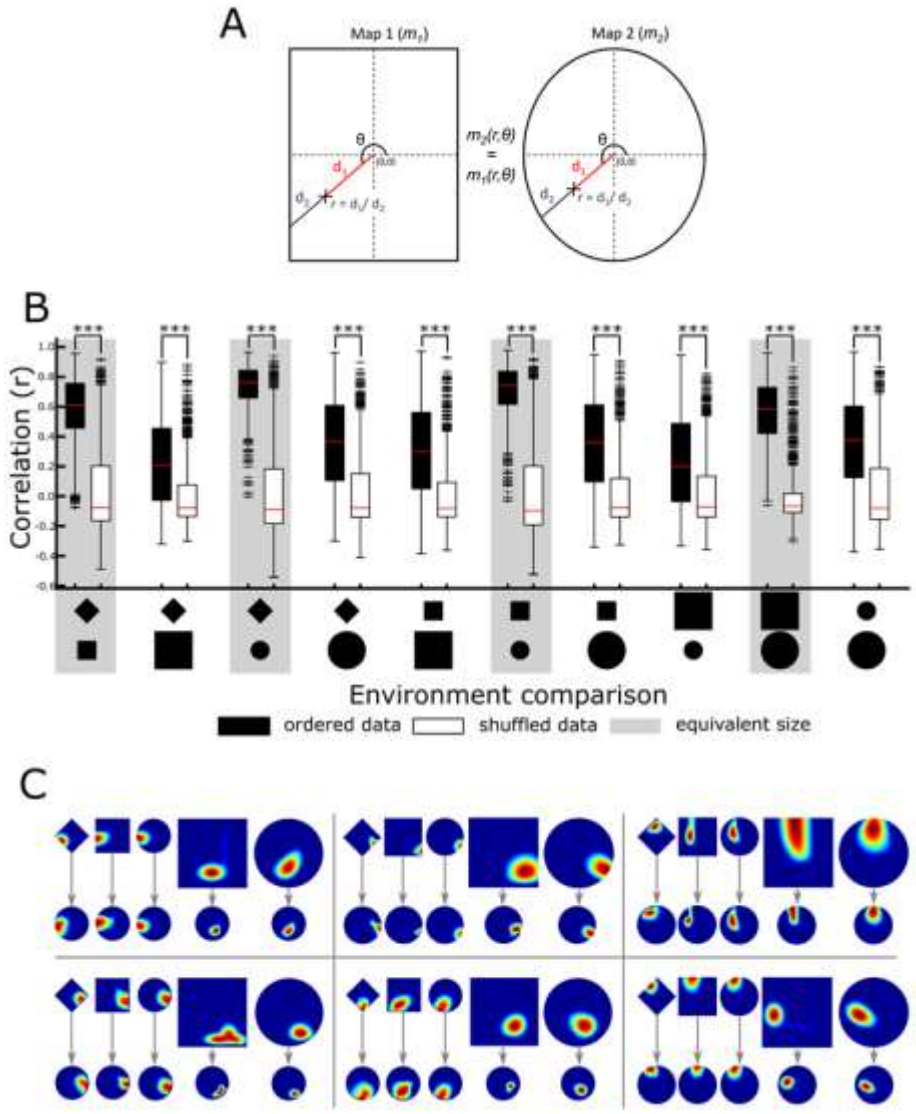

Figure 4 Place cell activity in the open field environments. ***A,*** schematic of the morphing procedure used. An inverse transformation is used to find pixels in map 1 which can best fill values in map 2, this is more efficient than the reverse process. ***B,*** distribution of values obtained by correlating the activity of a place cell in each open field environment to the same cell's activity in each other environment, after morphing the first to the same shape as the second. Open boxes indicate shuffled distributions where place cells were morphed and then compared to a random cell's activity in the second environment. Comparisons between environments which were initially the same size, not necessarily the same shape, are the highest (grey shaded comparisons), suggesting that place cells represent environments of corresponding size more similarly, regardless of their geometry. ***C,*** activity of six example cells, in each of the open field environments (top row) and result of morphing this activity to match the shape of the small circular environment (bottom row). Morphed versions of environments that are the initially the same size appear more similar than morphed versions of differently sized environments.

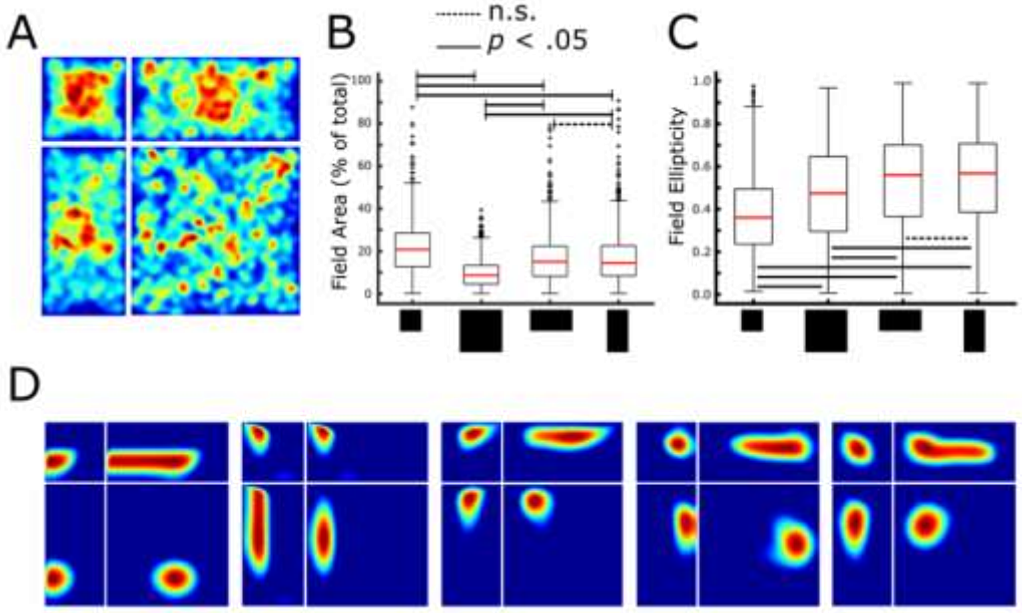

Figure 5 ***A,*** spatial maps of all place fields detected in the four square or rectangular environments. ***B,*** median size of place fields in each environment, expressed as a percentage of the environment's surface area. Fields do not expand to cover a similar proportion of the environment. ***C,*** median ellipticity of place fields in each environment. Place fields have a generally larger ellipticity in the rectangular environments, suggesting that they consistently expand with the environment. ***D,*** activity of four example place cells in all four square or rectangular environments. Each is seemingly sensitive to expansions of the environment in only one dimension.

Elongating an environment results in elongated place fields

The size of place fields differ significantly between the four rectangular and square mazes ($H(3,6469) = 964.5$, $p < 1 \times 10^{-200}$, Kruskal-Wallis test), post-hoc tests confirm that each environment differs from every other ($p < .0001$ in all cases) with the exception of the two rectangular environments ($p > .05$, Md = 15.0 and 14.5, all tests are Mann-Whitney U tests (MWUt) with a Bonferroni correction). The same relationship can be found when comparing place field ellipticity ($H(3,6469) = 574.6$, $p < 1 \times 10^{-120}$, Kruskal-Wallis test) and post-hoc tests again confirm that each environment differs from every other ($p < .0001$ in all cases) with the exception of the two rectangular environments ($p > .05$, Md = 0.56 and 0.57, all tests are MWUt with a Bonferroni correction). As with the previous open field analyses, we also find that place

fields do not expand in direct relation to the size of the environment; the observed ratio between the small square and rectangles is 1.6 (lower than the expected ratio of 2)(Figure 5).

A bisecting barrier increases place field repetition

In the square environment bisected by a barrier, we found that cells exhibited a significantly higher number of place fields than the same cells in a square open field environment of the same size (z = -24.6, p < .0001, r = -0.43, WRSt, Md = 1 in both cases). Specifically, in the square, cells are more likely to have a single place field, whereas in the insert maze cells were more likely to exhibit two fields. When comparing the half-map spatial correlations we also found that correlations from the barrier maze were significantly higher (D(3000) = 0.33, p < .0001, two-sample Kolmogorov-Smirnov test, Md = 0.24 and -0.07 respectively), suggesting that the doubling of place fields is a result of the bisecting barrier.

Discussion

As reported by Lever et al. (2002), our modelled place cells represent circle and square environments more similarly than would be expected by chance, but this effect is significantly decreased when the environments are of different sizes. The relationship between environment shape and size has not been expressly tested before, although Muller and Kubie (1987) report that when the diameter of a recording cylinder is enlarged, around 69% of cells are 'homotrophic' (i.e. their place field is of a similar size, shape and location relative to the walls). Lever et al. (2002) reported that in two similar sized but differently shaped environments 73% of place cells are homotrophic. Furthermore, when they removed the walls of their circular environment and allowed the animals to explore a larger circular platform, place cells fired much less similarly. This pattern of results clearly seems to follow the results of the current model; place cells represent environments of different shapes similarly, but this effect is stronger when they are also the same size.

As reported by O'Keefe and Burgess (1996), in a square environment that is enlarged along each dimension independently or both dimensions equally, place fields are significantly more elongated in the rectangular environments than in the squares. As above, we note that place fields in our larger environments are not merely scaled-up versions of the fields in the smaller ones. Muller and Kubie (1987) also reported the same effect in their data; depending on the methods used to generate their firing rate maps they found that, in a large cylinder that was twice the diameter of a small one (and 4 times the surface area), place fields only expanded their area by a factor of about two (values ranged from 0.87 to 2.49) which is very similar to our findings. Thus, place field area is not proportional to the area of the environment.

As reported previously by Barry and Burgess (2007), in a square environment bisected by a barrier, our modelled place cells exhibited more place fields than in a similarly sized open square. Furthermore, these cells were found to represent each half of the environment, as bisected by the barrier, more similarly than would be expected by chance. Together, these results confirm that our BVC model correctly predicts many of the geometric features of place cell firing observed in previous experiments.

Alleyway mazes

A number of experiments have demonstrated that in mazes composed of multiple alleyways, place cells exhibit place fields in similar locations along each alleyway. We propose that, in each case, the firing of place cells is repetitive due to the same process underlying firing in the square environment with a barrier insert. For instance, Frank et al. (2000) and Singer et al. (2010) recorded place cells in a maze composed of 2 to 6 repeating parallel alleyways. In these mazes, place cells expressed multiple place fields in a repeating fashion which was attributed to learning similar responses in different locations (Frank et al., 2000). However, the same phenomenon was observed when rats explored a maze composed of four parallel

alleyways for the first time, both in the light and in complete darkness (Grieves, 2015). As boundary cells respond similarly to vertical drops as they do to physical walls, it may be that their inputs can account for place field repetition in these types of mazes.

In another multialleyway experiment, Derdikman et al. (2009) showed that in a linear track composed of multiple alleyways that zig-zag back and forth through space, called a 'hairpin' maze, place cells exhibited place fields in similar locations along multiple alleys. However, they also found that these fields tended to occur at roughly the same distance along each alleyway and only in those alleyways which faced the same direction (i.e. in every second alleyway or in every alley where the rat faced south). This result is seemingly in contradiction to the BVC model as local geometry does not seem to change significantly between alleyways. Still, Derdikman et al. (2009) showed that field repetition persisted in rats trained in the same maze with transparent walls, but not in rats trained to run in a stereotypical manner in an open field, implicating the physical walls of the maze and thus local geometry.

In a similar demonstration of the importance of angular head direction, Nitz et al. (2011) found that, when rats run along a track which spirals inwards on itself, place cells often had multiple place fields positioned in different 'coils' of the spiral and arranged at a consistent angle with relation to the centre of the maze. As with the open field environments, we sought to replicate these findings in our modelled place cell population.

Methods

We modelled the activity of cells in a maze composed of four parallel alleyways as this best represented the mazes of Frank et al. (2000), Singer et al. (2010) and Grieves (2015). To quantify place field repetition, for each cell we calculated the spatial correlation between each pair of alleyways in the maze and compared this to a distribution of spatial correlation values calculated by comparing alleyway maps from different cells. This shuffle was performed without replacement. In all cases, a correlation was computed only if the firing rate in each alleyway

map was greater than 1 Hz. We also modelled the activity of place cells in a scale reproduction of the hairpin maze used by Derdikman et al. (2009) and in an open field environment of the same outer dimensions. We then performed a 1-dimensional autocorrelation whereby ratemaps were shifted laterally in 1 bin increments and correlated with themselves at each step. For the hairpin maze, in an analysis taken from Derdikman et al. (2009), we binned the place cell firing rate map using a pixel size of 15 cm (the width of an arm) × 10 cm (along the arm in the vertical dimension) and calculated the correlation between every possible pair of arms. These correlation values were compared to correlations obtained when, for each cell, the firing rate bins of each arm were shifted circularly by ± 150 cm or when the firing rate bins were reflected along the x-axis. In all cases, correlations were only performed when the firing rate of both arms was greater than 1 Hz. Finally, we modelled the activity of place cells in scale reproductions of the square and circular spiral mazes used by Nitz et al. (2011). We then found the angle of each place cell's fields relative to the centre of each environment, subtracted the circular median value from these and removed the value closest to zero (or a random value if multiple values were equally close to zero, which occurred if the circular median was the average of two values). This process automatically excludes data from cells with less than 2 fields. We also compared the angle of place fields between maze configurations.

Results

Place fields repeat in four parallel alleyways

As reported by Frank et al. (2000), Singer et al. (2010) and Grieves (2015), we observed a high level of place field repetition in the four alleyway maze, which can be seen in the peaks of the mean autocorrelation for all cells in this environment (Figure 6B). Arm correlation values were significantly higher on average than shuffled ones ($z = 75.3$, $p < .0001$, $r = 0.87$, WRSt, Md = 0.99 and < 0.001 respectively) (Figure 6C). Example place cells can be seen in Figure 6D.

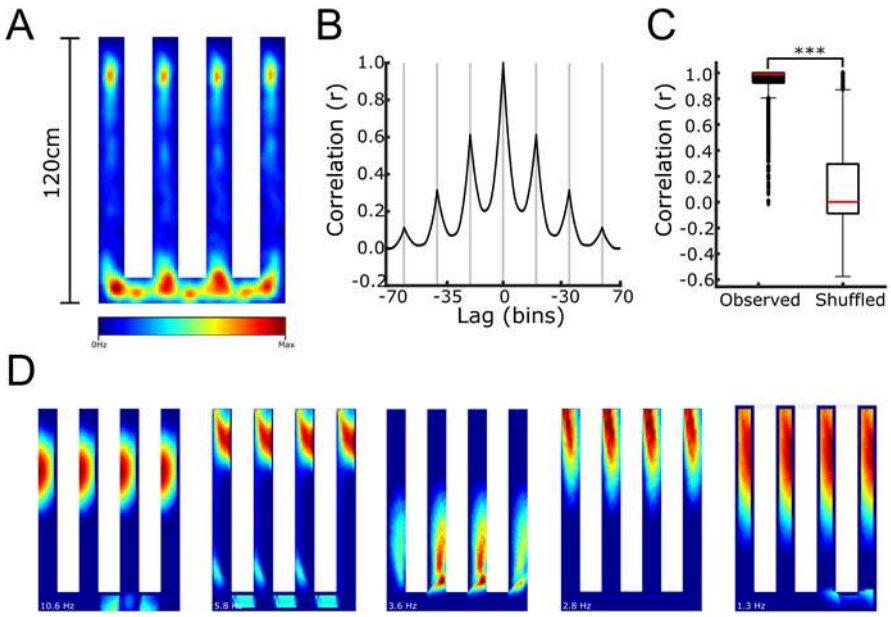

Figure 6 ***A,*** spatial map of all place fields detected in the four alleyway maze. ***B,*** mean and standard deviation linear autocorrelogram of all cells in the maze. Grey lines show the points at which alleyways overlap. ***C,*** median correlation either between arms of the maze (black box) or for a shuffled distribution where arms were compared to arm maps from other cells (open box). ***D,*** activity of five example place cells in this maze. Each exhibits repeating fields at similar locations along each alleyway. The number of BVC inputs these cells receive increases from left to right (2,3,4,6 and 7 inputs).

Place fields repeat in a hairpin maze and turning points are overrepresented

A different proportion of cells were active (firing > 1Hz) in our hairpin maze when compared to an open field environment of the same size (1477 or 98.47% and 1202 or 80.13% respectively; $x^2(1) = 28.23$, $p < .0001$, $\varphi_c = 0.02$, Chi-square test) and these cells also exhibited a much higher number of fields in the hairpin maze ($z = 49.3$, $p < .0001$, $r = 0.82$, WRSt, Md = 10 and 1 respectively). The spatial distribution of place fields was also very different in these two mazes. When comparing the top 37.5cm and bottom 37.5cm sections of the hairpin maze to the middle 75cm zone, the majority of place fields in the hairpin maze were found in the top and bottom sections (11084 (72%) and 4368 (28%) respectively; $x^2(1) = 2919$, $p < .0001$, $\varphi_c = 0.19$, Chi-square test); this effect was not observed in the open field (845 fields (50%) and 853 fields (50%) respectively, $x^2(1) = 0.04$, $p > .80$, $\varphi_c < 0.01$, Chi-square test) (Figure 7A, B and C).

Horizontal autocorrelations of the hairpin maze firing rate maps display clear peaks at a shift of 0 (where the map overlaps with itself) but also at intervals of 30 bins (30 cm) where alleyways with the same orientation overlap. Smaller peaks can also be seen at intervals of 15 bins (15 cm) where differently oriented alleyways overlap. Correlation values are higher at 30 bin than 15 bin intervals ($z = 51.1$, $p < .0001$, $r = 0.31$, WRSt, Md = 0.41 and 0.26 respectively) and both are higher than corresponding values in autocorrelations performed on the open field environment ($z = 113.7$, $p < .0001$, $r = 0.68$, Md = 0.41 and 0.0 respectively; $z = 82.3$, $p < .0001$, $r = 0.31$, Md = 0.26 and 0.0 respectively, WRSt) (Figure 7D). The mean autocorrelogram for each place cell shows a consistent effect throughout the vast majority of our place cells which does not seem to be affected by the number of BVC inputs a place cell receives (Figure 7E).

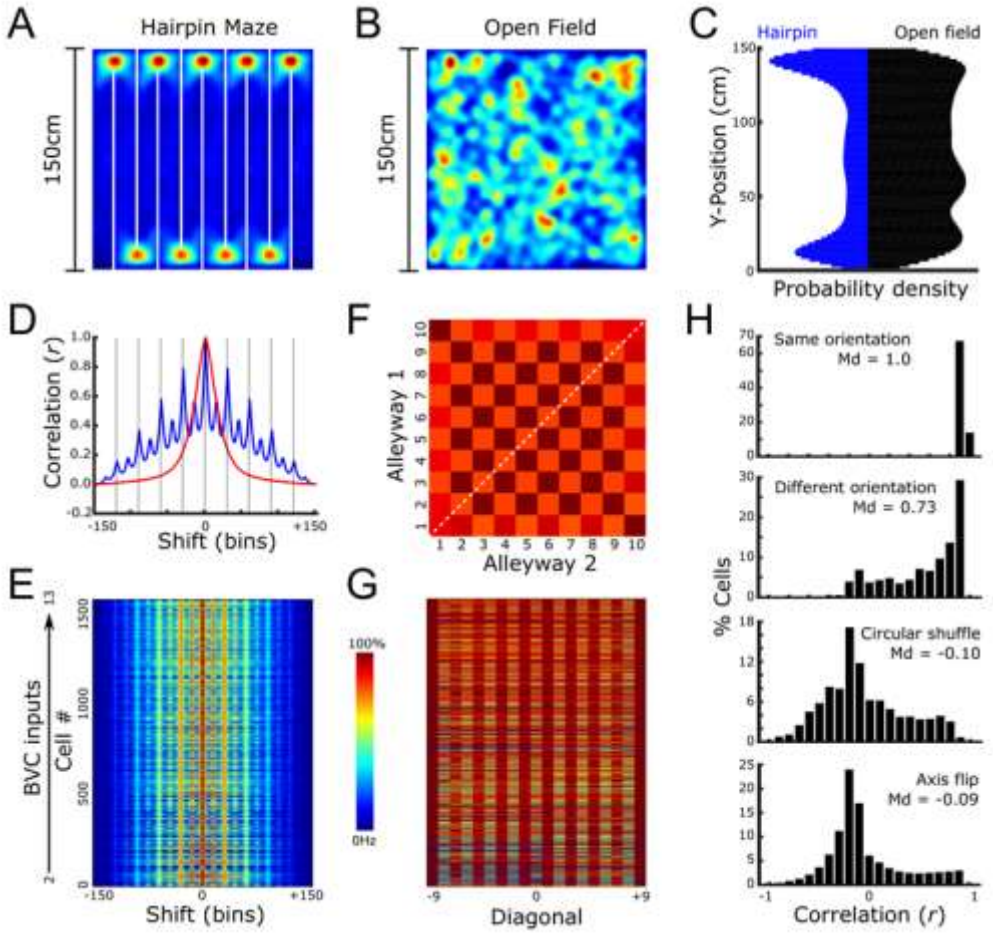

Figure 7 Place cell activity in the Derdikman et al. (2009) apparatus. ***A,*** spatial map of all place fields detected in the hairpin maze. ***B,*** spatial map of all place fields detected in an open field with the same outer dimensions as the hairpin maze. ***C,*** violin plot showing the distribution of place fields along the y-axis in both the hairpin and open field apparatus. ***D,*** mean and standard deviation linear autocorrelogram of all cells in the hairpin maze (blue line) and in the open field (red line). Dotted lines show where the shifted hairpin maze alleyways line up with alleyways facing the same direction. ***E,*** linear autocorrelogram of all 1500 cells in the hairpin maze, one per row, these are arranged from cells with few to most BVC inputs. ***F,*** mean correlation matrix of all cells, each bin represents a comparison between two alleyways of the hairpin maze. The checkerboard pattern here resembles that reported by Derdikman et al. (2009) and indicates that those alleyways separated by an odd number of alleyways (i.e. alleyways facing the same direction) are more highly correlated. ***G,*** diagonal mean of each cell's correlation matrix, taken along the white dotted line shown in F, one cell per row, these are arranged as in E. ***H,*** distribution of correlation values obtained when comparing alleyways. The top graph shows the distribution when comparing odd or even alleyways (i.e. facing the same direction), the second graph shows the distribution when comparing odd to even alleyways (i.e. facing different directions), the third graph shows the distribution when comparing alleyways facing different directions after circularly rotating all odd numbered alleyways by a random number of bins and the bottom graph shows the distribution when comparing alleyways facing different directions after rotating all odd numbered alleyways 180^{o} around their centre.

Fields repeat only in alternating (odd or even) arms

As reported by Derdikman et al. (2009), when we observed the results of arm correlations as a matrix, a clear checkerboard pattern emerged, consistent with higher correlation values for same orientation alleyways compared to different orientation ones (Figure 7F). In agreement with this, correlation values for same orientation alleyways were higher (z = 246.6, $p < .0001$, r = 0.60, WRSt, Md = 1.0 and 0.73 respectively). They were also higher than shuffled distributions where each arm was randomly shuffled circularly (z = 310.6, $p < .0001$, r = 0.88, WRSt, Md = 1.0 and -0.10 respectively) or where alternating arms were reflected along the x-axis (z = 247.6, $p < .0001$, r = 0.87, WRSt, Md = 1.0 and -0.09 respectively)(Figure 7H). Again, the mean diagonal of each cell's correlation matrix shows that this effect was consistent throughout most place cells, and the number of BVC inputs a place cell receives did not seem to affect this (Figure 7G). Example BVCs and place cells can be seen in Figure 8.

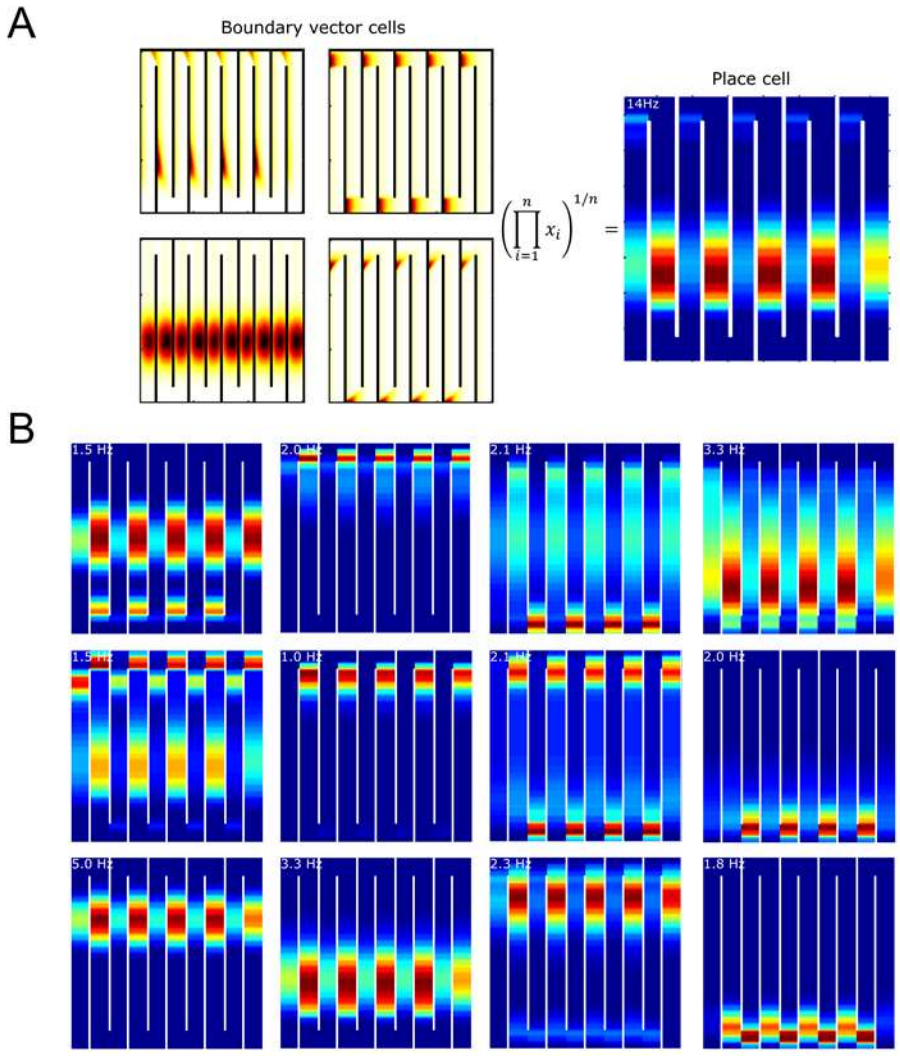

Figure 8 Place cell activity in the Derdikman et al. (2009) apparatus. ***A,*** activity of four example BVCs in the hairpin maze (left) and activity of the place cell generated exclusively from these inputs (right). ***B***, the activity of 12 more place cells in the hairpin maze, each exhibits repeating fields at similar locations along multiple alleyways that face the same direction. The number of BVC inputs these cells receive increases from top to bottom and from left to right (2 to 13 inputs; 13 inputs was the maximum utilised and only by one cell).

Place cell characteristics are similar in a square and circular spiral, but fields in the circular spiral get larger as loop size increases

In the two spiral mazes we observed a different proportion of active (firing > 1Hz) cells, but this was accompanied by a low effect size (1295 or 13.67% and 1418 or 5.47% respectively; $x^2(1) = 5.48$, $p < .02$, $\varphi_c = 0.04$, Chi-square test). Cells also exhibited a different number of fields

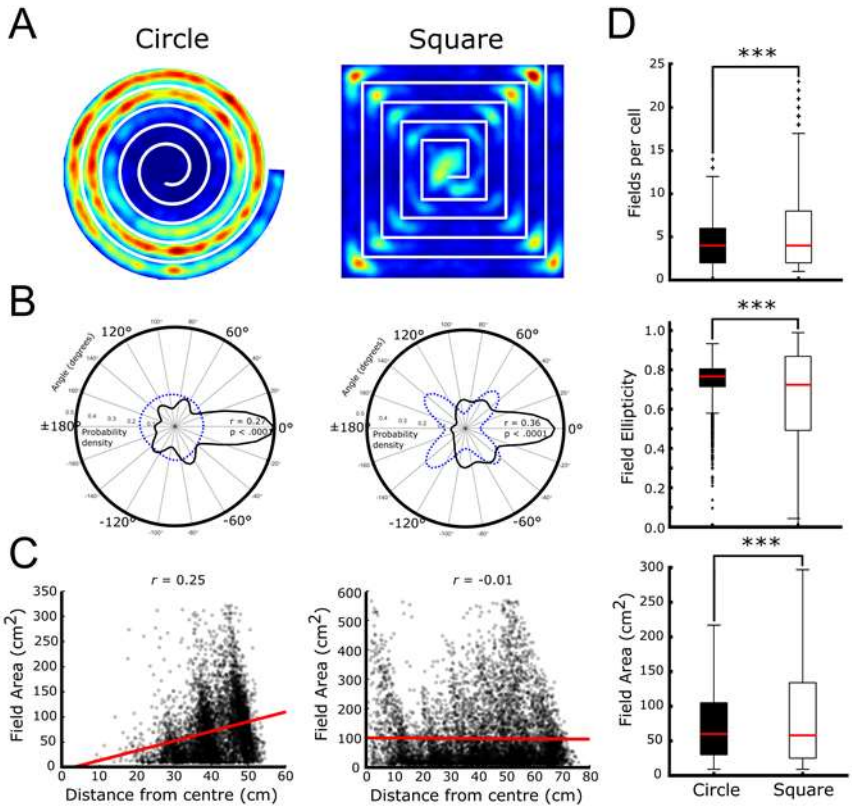

Figure 9 Place cell activity in the Nitz (2011) apparatus. ***A,*** spatial map of all place fields detected in the spiral mazes. ***B,*** circular polar plots showing the position of all place fields in the circular spiral (left) and square spiral (right). This is expressed as the field's angle from the centre of the apparatus (blue dotted line) or when the median field angle for each cell is subtracted from all of its fields' values (black line). For the black line, an accumulation of fields around zero indicates that each place cell's fields lie on a radial line from the centre of the maze to the edge. ***C,*** density scatter graphs showing the size of all detected place fields in relation to their distance from the centre of the maze. ***D,*** boxplots showing place field statistics for the circular spiral (black boxes) and square spiral (open boxes). The top plot shows the median number of place fields per cell, the second plot shows the median ellipticity and the bottom plot shows the median place field area.

in each maze, but again with a low effect size (z = 3.3, p < .0001, r = 0.06, WRSt, Md = 4 in both cases) (Figure 9D). Place fields were generally more elliptical in the circular maze than the square one (z = 10.5, p < .0001, r = 0.23, WRSt, Md = 0.77 and 0.72 respectively) (Figure 9D). Fields were also slightly larger in the circular maze (z = -2.1, p < .05, r = -0.11, WRSt, Md = 60 and 58cm^2 respectively) and fields increased in size linearly as the distance from the maze

centre increased ($r(6479) = 0.25$, $p < .0001$), although not for fields in the square maze ($r(7978) = -0.01$, $p > .30$) (Figure 9C).

Repeating fields are often found on a line from the centre of the spiral, turning points in the square spiral are overrepresented

In both the circular and square maze, fields were not unimodally distributed around the centre ($r = 0.04$ and $r = 0.06$ respective Rayleigh vector tests). Moreover, when comparing the frequency of fields at 90^o offsets to those at 45^o offsets we found that, in the square maze, significantly more fields were distributed along 45^o offsets than 90^o ones ($t(6) = 14.9$, $p < .0001$) reflecting the geometry of the maze. The same relationship was not observed in the circular maze fields ($t(6) = -0.7$, $p > .50$, Figure 9B dashed blue lines). As reported by Nitz et al. (2011), these results are in agreement with field clustering in the corners of the square maze alleyways and can also be seen in a heatmap of all place fields on each maze (Figure 9A). However, when we subtracted the median angle from each cell's field angles, the results clustered around zero in both mazes ($r = 0.27$ and $r = 0.36$ respective Rayleigh vector tests; $v = 1337$, $p < .0001$ and $v = 2310$, $p < .0001$ respective non-uniformity V-tests, Figure 9B solid black lines). This confirms that the majority of cells in these mazes have place fields which fall on a line from the centre of the maze once their median angle is subtracted. Furthermore, when comparing the field angles of cells in the two maze configurations the resulting correlation was significant ($r(452) = 0.17$, $p < .0005$, Spearman's pairwise correlation) and the values were more similar than would be expected by chance ($z = -5.0$, $p < .0001$, Wilcoxon signed rank test, Md = 39.68), indicating that cells exhibited fields in similar locations on the two mazes. Example BVCs and place cells can be seen in Figure 10.

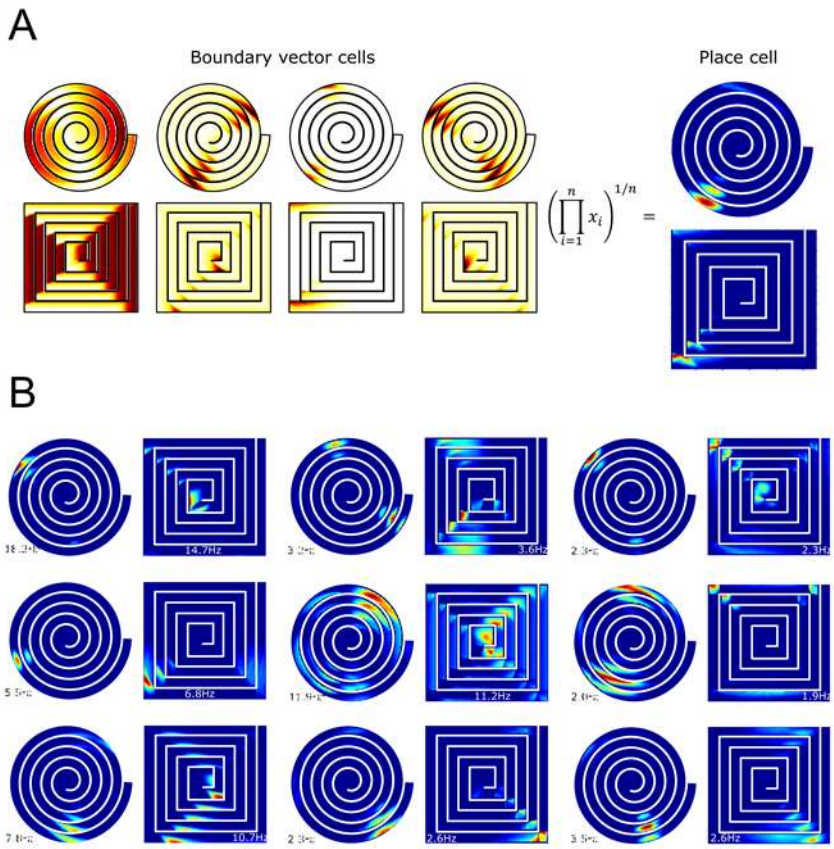

Figure 10 Place cell activity in the Nitz (2011) apparatus. ***A,*** the activity of four example BVCs in the spiral mazes (left) and the activity of the place cell generated exclusively from these inputs (right). ***B,*** the activity of 9 more place cells in the spiral mazes, each exhibits repeating fields that fall on a line drawn from the centre of the maze to the edge. The number of BVC inputs these cells receive increases from top to bottom and from left to right (2 to 10 inputs; 13 inputs was the maximum utilised and only by one cell).

Discussion

We modelled the activity of place cells in a maze composed of four parallel alleyways, and predicted that BVCs and modelled place cells would respond identically in each. This was the case, confirming that activity does not require experience or learning to develop, and that it can be explained by a geometric model of place cell firing.

As reported by Derdikman et al. (2009), in a multi-alleyway hairpin maze, modelled place cells exhibited repeating fields only in alleyways with the same orientation. Furthermore, the representations in alternating alleyways were not merely mirror images of each other,

confirming that a geometric model of place cell firing can account for this effect despite the very small geometric change between alleyways. We also observed an overrepresentation of place fields at the ends of the alleyways (i.e. at the turning points between alleyways). This seemed to be due to the higher probability of BVC activity overlapping there and although not reported, was one of the effects observed in the original study (D. Derdikman, personal communication). One feature of the original data that the current model cannot support is the fact that place cells in the original study exhibited completely different representations for left-right trajectories through the maze compared to right-left trajectories. This effect can be thought of as analogous to place field directionality in a linear track (McNaughton, Barnes, & O'Keefe, 1983) and is unexplained by the current model, unless we consider that BVCs and place cells initialise a new map for each running direction. A BVC model incorporating visual inputs (Raudies & Hasselmo, 2012), learning (Navratilova, Hoang, Schwindel, Tatsuno, & McNaughton, 2012) or contextual information (Hayman & Jeffery, 2008) may better explain this effect.

Lastly, as reported by Nitz (2011) we found that, in a spiral maze, the majority of modelled place cells exhibited repeating place fields, generally falling on a ray drawn from the centre of the maze to the edge (i.e. appearing in multiple loops of the spirals where the rat faced the same direction). Modelled place cells also exhibited firing features in common with the observations of Nitz (2011). For instance, cells did not necessarily exhibit fields on all loops (many cells did not have fields in the first or last loops) and fields in the square spiral track were more elongated than those in the circular spiral. In the circular spiral maze, field area was also strongly correlated with loop size (measured as distance from the maze centre) but in the square maze this correlation was absent. Many cells in the square maze exhibited fields in the corners of the square spiral that did not adapt their area to the size of the loop. This last result simply seemed to be due to the higher probability of BVC inputs overlapping in the corners, where two or more cells with near-perpendicular preferred firing directions can intersect. Lastly,

when comparing the square and circular spirals, place fields seemed to be present at the same angle relative to the centre of the spiral in both mazes.

Nitz (2011) suggested that the BVC model could not explain the repeating fields observed in these spiral mazes because cells should have fields in every loop. However, he also pointed out that in the vast majority of these cases the missing field was located on the far most outer or inner loops and we saw this same effect in our modelled data. This was probably due different BVCs having different firing characteristics, meaning that while the activity of a set of BVCs projecting to a place cell may overlap in several adjacent loops, this overlap diminishes as the geometry of the loop diverges. Thus, the firing rates of adjacent place fields form a curve, sloping downwards from the loop where BVC inputs combine most effectively. If this is centred on a central loop then fields will be weaker or completely absent in more distant (i.e. inner and outer) loops. Taken together, these results demonstrate that the BVC model does not need to incorporate head direction or response sequences to explain place cell firing in spiral mazes.

Multicompartment mazes

Our primary hypothesis was that the place field repetition observed by Spiers et al. (2015) in four parallel and visually identical compartments, as well as the absence of place field repetition observed by Grieves et al. (2016b) in the same compartments when they were angled away from each other, can be explained in terms of BVC inputs to hippocampal place cells. Our prediction was that these same effects would be observable in a model of place cell firing based solely on geometric inputs from BVCs. As earlier potential examples of place field repetition were observed across mazes with two compartments, we also modelled two compartments connected by a corridor (parallel; Skaggs and McNaughton (1998)) and two compartments connected end to end (north to south; Tanila (1999). Together, these environments are comparable to the environments used by Fuhs et al. (2005).

Methods

For the two compartment mazes, we used analyses described by Fuhs et al. (2005). Firstly, we calculated the spatial correlation between the two compartments in the corridor version of the task and between the two compartments in the opposite version (Figure 11A). For the opposite configuration, we conducted analyses both with the bottom compartment rotated 180° or left unrotated. We also calculated compartment by compartment spatial correlations between the two mazes, again both with the bottom compartment in the opposite configuration rotated 180° or left unrotated. For each comparison, we also calculated an equivalent measure between random cells without replacement. In all cases, a correlation was computed only if the firing rate in each map was greater than 1 Hz. We also calculated the correlation between maximum firing rates (peak value in the ratemap) in both compartments for each maze.

We note that the compartments in the opposite configuration of Fuhs et al. (2005) were each rotated $\pm$90° relative to their counterpart compartments in the parallel configuration. However, rats likely relied on local cues to orient themselves when placed in each maze configuration, as both mazes were placed in the same curtained enclosure which did not contain distal cues and the lighting was maintained evenly throughout environments. Fuhs et al. (2005) reported that place cells from the majority of rats represented compartment 1 similarly in each maze configuration if ratemaps for compartment 1 in the opposite configuration were first rotated 90 degrees to match the parallel configuration. This suggests that when rats were first introduced to the opposite configuration (always after experiencing the parallel configuration) they oriented themselves using the first experienced compartment and visual cue. Thus, we maintained the orientation of our modelled BVCs in each compartment 1, which is equivalent to rotating Fuhs et al.'s (2005) parallel configuration maze +90 degrees. This is reflected in the orientation of maps in Figure 11A.

For the four compartment mazes we replicated the analyses used by Spiers et al. (2015) and Grieves et al. (2016b). Firstly, we calculated the spatial correlation between each

559 compartment in the parallel maze to every other compartment. We did the same for the radial
560 maze but with all of the compartments rotated so that their longest axis was vertical, as in the
561 parallel maze, before correlating them. For comparison, we also conducted the same analysis
562 on pairs of maze compartments from random cells (where compartment identity was
563 maintained). We did this without replacement. We also performed a 1-dimensional lateral
564 autocorrelation on compartment firing rate maps concatenated edge to edge to form a single
565 map and we counted the number of place fields observed per cell in each environment. Lastly,
566 we calculated the spatial correlation between compartments in the two mazes (i.e. compartment
567 1 in the parallel maze vs compartment 1 in the radial maze) and for comparison we calculated
568 this correlation when the cells were shuffled but compartment identity was maintained. This was
569 also done without replacement. In all cases, a correlation was computed only if the firing rate in
570 each map was greater than 1 Hz. In both maze configurations, we observed a high number of
571 place fields in the doorways. To test if more fields were observed there than could be expected
572 by chance, we counted the number of fields found in the four doorway zones and compared this
573 number to those found in four equally sized zones distributed randomly throughout the
574 environment. We did this 1000 times, with control zones that were confined within the walls of
575 the maze and that could overlap.
576 One potential criticism of the analysis used by Grieves et al. (2016b) is that by rotating
577 the compartments in the radial configuration of the maze the relationship between boundaries
578 and place fields was disrupted, thus lowering any potential correlation in that maze. However,
579 Grieves et al. (2016b) detected place fields in their mazes and found an average of 1.12 (SEM =
580 0.06) place fields per cell in the radial configuration of their maze but 2.18 fields per cell (SEM =
581 0.18) in the parallel configuration (Grieves, 2015), suggesting that cells have more fields in the
582 parallel version rather than just repositioned fields in the radial maze. Nevertheless, to test this
583 hypothesis in our place cell population, we conducted the analyses described above on

584 ‘morphed’ or reshaped radial maze compartments instead of rotating them, using the morphing
585 algorithm previously described in overall methods.

586 **Results**

587 *Place fields repeat in two parallel compartments but not in two opposite ones*

588 As reported by Fuhs et al. (2005), correlations between parallel compartments were
589 much higher than between opposite compartments. This was the case whether we rotated the
590 bottom compartment in the opposite configuration 180° ($D(3000) = 0.96$, $p < .0001$, two-sample
591 Kolmogorov-Smirnov test, Md = 0.99 and -0.09 respectively) or not ($D(3000) = 0.72$, $p < .0001$,
592 two-sample Kolmogorov-Smirnov test, Md = 0.99 and 0.60 respectively). However, without
593 rotation we did see a significant increase in correlation values ($D(3000) = 0.58$, $p < .0001$, two-
594 sample Kolmogorov-Smirnov test, Md = -0.09 and 0.60 respectively) (Figure 11B). Firing rates
595 in the parallel configuration compartments were also more highly correlated than those in the
596 opposite configuration ($r(1498) = 0.84$, $p < .0001$ and $r(1498) = 0.55$, $p < .0001$ respective
597 Spearman’s correlations) (Figure 11D).

598

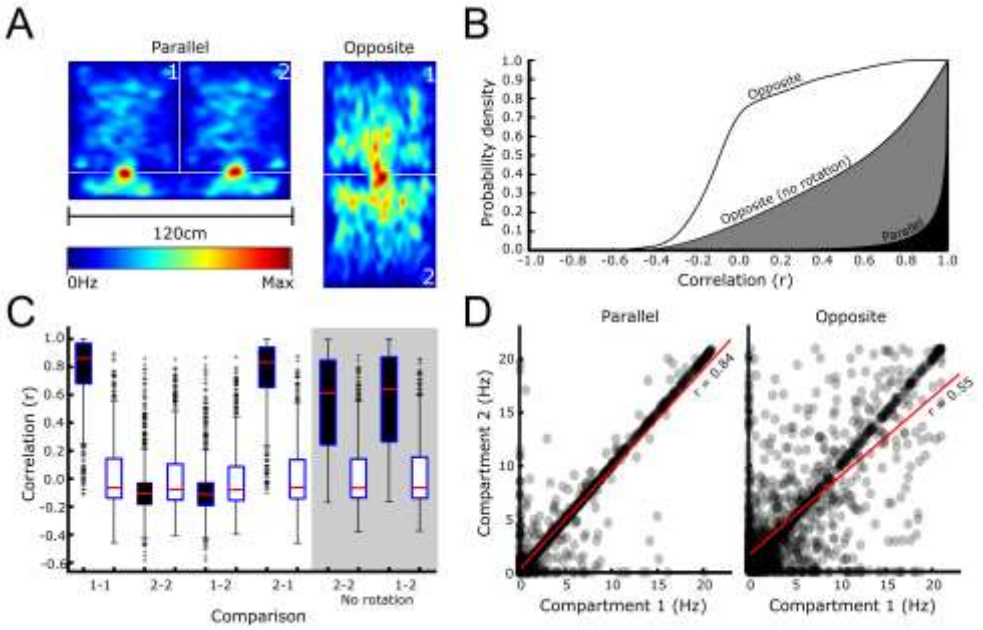

Figure 11 Place cell activity in the Fuhs et al. (2005) apparatus. ***A,*** spatial maps of all place fields detected in the two configurations of the maze. ***B,*** cumulative probability density functions for the correlation distributions found when comparing the compartments within each maze. Black shows the distribution when comparing compartments in the parallel configuration, white shows the distribution when comparing compartments in the opposite configuration after rotating compartment 2 by 180^{o} to match compartment 1, grey shows the distribution when comparing compartments in the opposite configuration without rotating compartment 2. ***C,*** correlation distributions found when comparing compartments between the two maze configurations (i.e. compartment 2 in the parallel configuration to compartment 1 in the opposite configuration). The left eight boxes show the distributions after rotating compartment 2 in the opposite configuration by 180^{o}, the four right boxes (on a grey background) show distributions without this rotation. ***D,*** density scatter plots showing the correlation (red line) between compartment firing rates (maximum in compartment ratemap) in the parallel (left plot) and opposite (right plot) maze configurations.

Cells exhibit a distinct representation for the opposite compartment

The four possible comparisons we made between the two mazes resulted in significantly different correlation distributions whether compartment 2 in the opposite configuration was rotated ($H(3,3532) = 2461$, $p < .0001$, Kruskal-Wallis test) or not ($H(3,3532) = 410.4$, $p < .0001$, Kruskal-Wallis test). In either case, post-hoc tests confirmed that each distribution differed from every other ($p < .0001$ in all cases) except comparisons between either parallel compartments 1 and 2 and opposite compartment 1 which were equally high ($p > .05$, Md = 0.86 and 0.83) and comparisons between either parallel compartments 1 and 2 and opposite compartment 2 which were equally low (with rotation: $p > .05$, Md = -0.10 and -0.11; without rotation: $p > .05$, Md = 0.61 and 0.64). Note that, when we rotated compartment 2 in the opposite configuration, the correlation between this and compartments 1 and 2 in the parallel configuration decreased. Indeed, this decrease was statistically significant for each ($p < .0001$ and $r > 0.70$ in both cases, WRSt). These effects can be seen in Figure 11C. All distributions differed significantly from their shuffled distributions ($p < .05$ in all cases WRSt) but with varying effect sizes (with rotation: r = 0.83, 0.83, -0.16, and -0.17; without rotation: r = 0.82, 0.64, 0.65 and 0.82). Shuffled distributions did not differ whether compartment 2 was rotated ($H(3,2989) = 6.91$, $p > .05$, Kruskal-Wallis test) or not ($H(3,2975) = 0.89$, $p > .80$, Kruskal-Wallis test) (Figure 11C). Example BVCs and place cells can be seen in Figure 12.

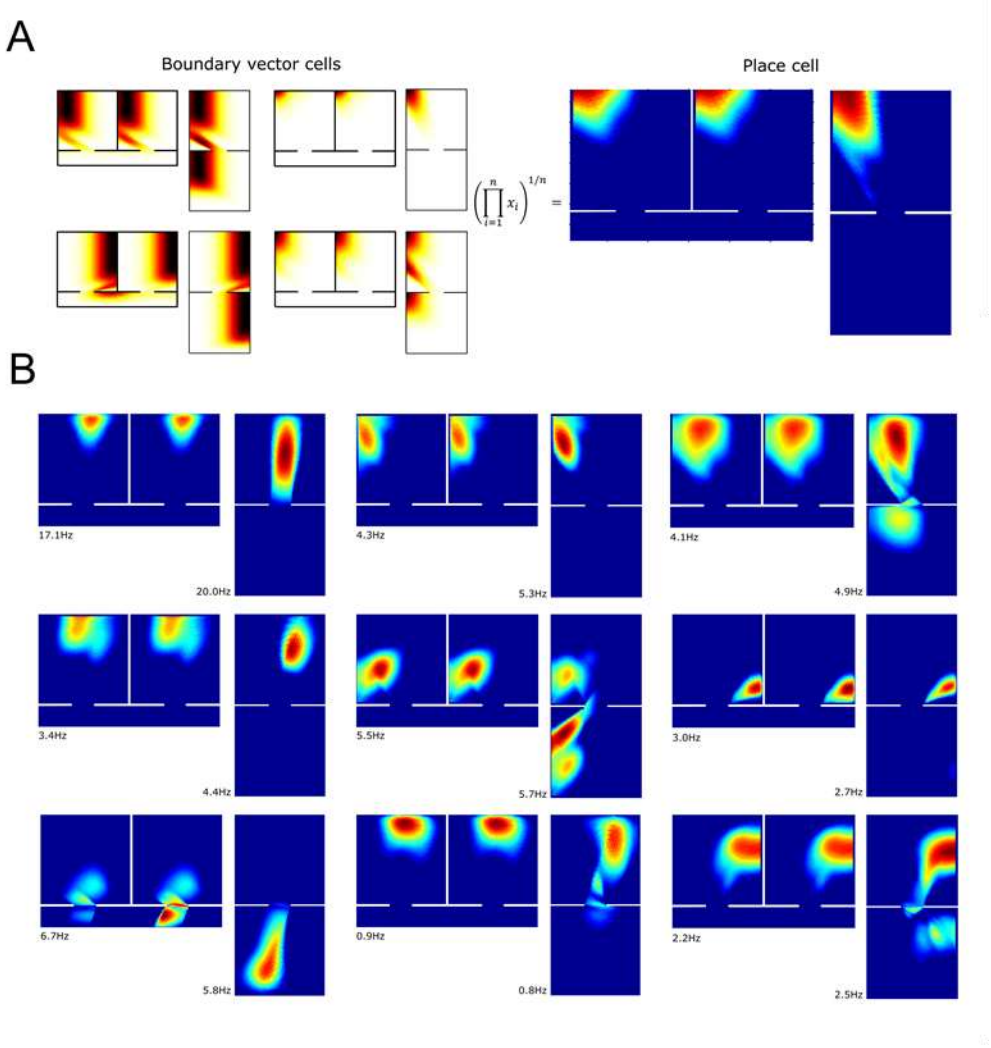

Figure 12 Place cell activity in the Fuhs et al. (2005) apparatus. ***A,*** activity of four example BVCs in the two compartment mazes (left) and activity of the place cell generated exclusively from these inputs (right). ***B,*** activity of 9 more place cells in the two compartment mazes, each exhibits repeating fields. The number of BVC inputs these cells receive increases from top to bottom and from left to right (2 to 10 inputs; 13 was the maximum utilised and only by one cell).

Cells exhibit more fields in four parallel compartments than four radial ones, and many of these are in doorways

In the four compartment mazes we observed a similar proportion of active (firing > 1Hz) cells in the parallel and radial configurations (1294 or 86.27% and 1302 or 86.80% respectively; $x^2(1) = 0.03$, $p > .80$, $\varphi_c < 0.01$, Chi-square test). The number of place fields exhibited per cell in each environment was significantly different, however, with a much higher number of fields

being exhibited by cells in the parallel configuration of the maze (z = 18.26, p < .0001, r = 0.31, WRSt, Md = 4 and 2 respectively) (Figure 13E). In the parallel maze, 762 place fields (12.21%) were observed in the four doorways. This number was significantly higher than the distribution obtained from the random control points (99th percentile = 369, Md = 160, kernel smoothed density estimated $p = 1.16 \times 10^{-41}$). The same effect was observed in the radial maze where 543 place fields (13.13%) were observed in the four doorways, significantly higher than in the random control points (99th percentile = 302, Md = 79, kernel smoothed density estimated $p = 3.8 \times 10^{-25}$).

Place cells repeat the same representation in four parallel compartments, but not in four radial ones

In the parallel maze, clear autocorrelation peaks can be seen at a shift of 0 but also at intervals of 35 bins (35 cm) where different compartments overlap. Correlation values were higher at 35 bin than 17.5 bin intervals (z = 82.5, p < .0001, r = 0.67, WRSt, Md = 0.49 and 0.01 respectively) and they were higher than corresponding values in autocorrelations performed on the radial configuration (z = 63.9, p < .0001, r = 0.39, WRSt, Md = 0.01). In the radial data, values at 35 bin intervals were also higher than those as 17.5 bin intervals but this was accompanied by a lower effect size (z = 16.5, p < .0001, r = 0.28, WRSt, Md = 0.01 and 0.01 respectively) (Figure 13C). In the mean autocorrelogram for each place cell, this effect appeared consistent throughout the vast majority of place cells and the number of BVC inputs a place cell receives did not seem to affect this (Figure 13B).

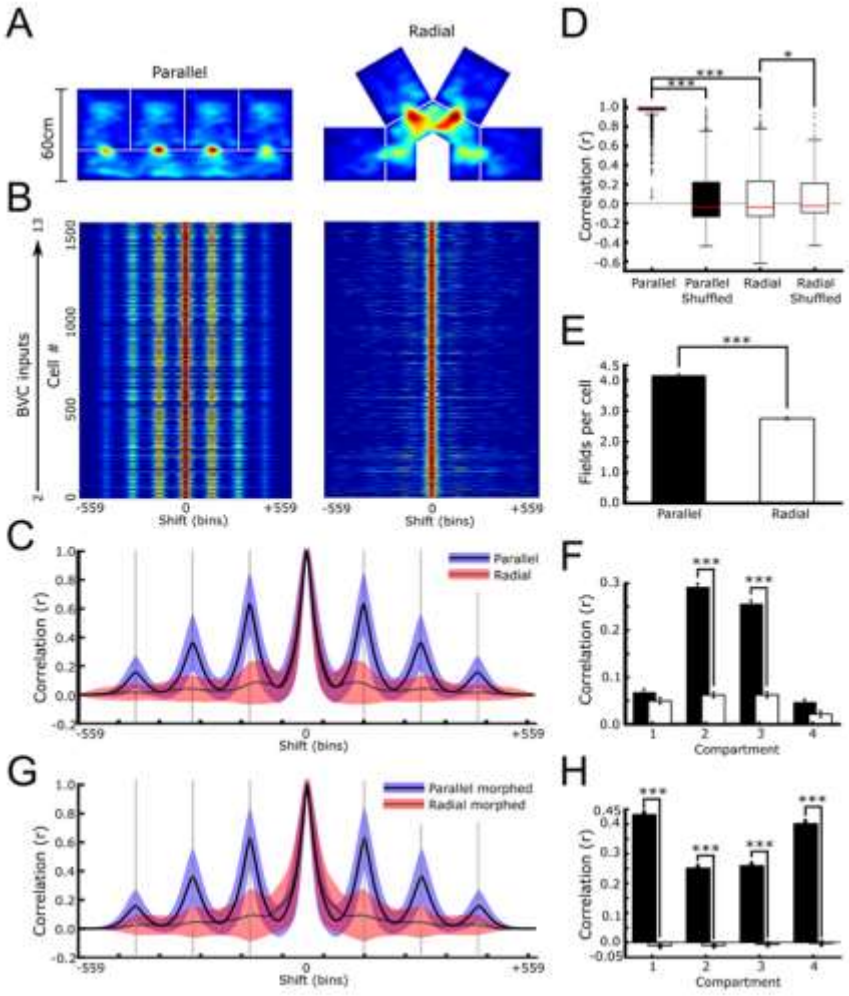

Figure 13 Place cell activity in the four compartment mazes used by Grieves et al. (2016) and Spiers et al. (2015). ***A,*** spatial map of all place fields detected in the parallel (left) and radial (right) configuration of the maze. ***B,*** the linear autocorrelogram of all 1,500 cells in the parallel (left) and radial (right) configurations, one per row, arranged from cells with few to most BVC inputs. ***C,*** mean (black lines) and standard deviation (shaded areas) linear autocorrelogram of all cells in the parallel (solid line and blue area) and radial (dashed line and red area) mazes. A periodicity can be observed in the parallel autocorrelation but not in the radial, as reported by Grieves et al. (2016). ***D,*** within-maze compartment correlation distributions (black boxes) and the distributions obtained using shuffled compartment ratemaps (open boxes). The distributions are all centred on zero, with the exception of the distribution obtained from the parallel maze. ***E,*** average and SEM number of place fields per cell observed in each maze. ***F,*** between-maze compartment correlation distributions (black bars) and distributions obtained after shuffling these compartments (open bars). Only the correlations between compartments 2 and 3 are significantly above chance, these compartments are the most similarly oriented between the two mazes, with a 30^{o} offset. ***G,*** same as C, but for morphed instead of rotated data. ***H,*** same as F but for morphed instead of rotated data. In this case, all compartments have significant correlations.

We next computed between-compartment correlations in the parallel and radial configuration and a shuffled distribution for each. These differed significantly ($H(3,7145) = 5060$, $p < .0001$, Kruskal-Wallis test) and post-hoc tests confirmed that parallel maze values were significantly higher than the other three distributions ($p < .0001$ in all cases, Md = 0.99, -0.04, -0.04 and -0.03 respectively). However, the shuffled parallel, radial and shuffled radial distributions were all similarly low ($p > .90$ in all cases)(Figure 13D). Inter-maze comparisons (i.e. compartment 1 in parallel configuration vs compartment 1 in the radial configuration) were not homogenous ($H(3,1572) = 200.4$, $p < .0001$, Kruskal-Wallis test). Post-hoc tests confirmed that each distribution differed from every other ($p < .0001$ in all cases) with the exception of comparisons between compartments 1 and 4, which were equally low ($p > .05$, Md = -0.03 and -0.04), and comparisons between compartments 2 and 3, which were equally high ($p > .05$, Md = 0.30 and 0.21). When compared independently to shuffled distributions, only comparisons between compartments 2 and 3 were significantly above chance ($z = 1.48$, $p > .10$, $r = 0.06$, $z = 12.02$, $p < .0001$, $r = 0.41$, $z = 10.47$, $p < .0001$, $r = 0.36$ and $z = -0.28$, $p > .70$, $r = -0.03$, respective WRSts, Figure 13F). Example BVCs and place cells can be seen in Figure 14.

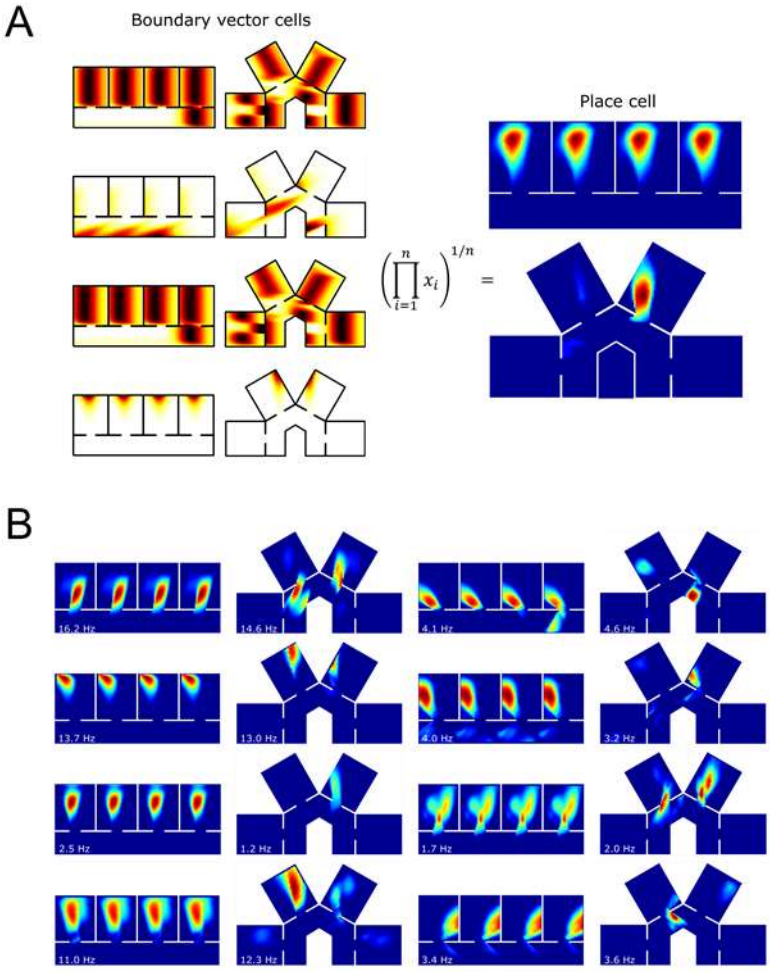

Figure 14 Place cell activity in the Grieves et al. (2016) and Spiers et al. (2015) apparatus. ***A,*** activity of four example BVCs in the two maze configurations (left) and activity of the place cell generated exclusively from these inputs (right). ***B,*** activity of 8 more place cells in these mazes, each exhibits repeating fields in the parallel configuration but not in the radial one. The number of BVC inputs these cells receive increases from top to bottom and from left to right (2 to 9 inputs; 13 was the maximum utilised and only by one cell).

Rotating compartment maps decreases the correlation between them, but morphed radial maze compartments are still less similar than parallel ones

Correlations between mazes suggest that the compartments rotated by the least amount (2 and 3 are rotated +30º and -30º, 1 and 4 are rotated +90º and -90º respectively) correlate more highly. To test whether rotation itself results in lower correlations, we morphed compartments in the radial configuration instead of simply rotating them. We also morphed the

parallel configuration maps but for this maze no statistical values differed from the rotated data described above. Next, we performed a horizontal autocorrelation on concatenated compartment ratemaps. In contrast to above, the morphed radial data values at 35 bin intervals were not higher than those at 17.5 bin intervals (z = 1.84, p > .06, r = 0.22, WRSt, Md = 0.01 and 0.01 respectively)(Figure 13G). We then computed between-compartment correlations in the parallel and radial configuration and a shuffled distribution for each. The resulting distributions differed significantly (H(3,7236) = 5130.7, p < .0001, Kruskal-Wallis test) and post-hoc tests confirmed that each distribution differed from each of the others (p < .0001 in all cases), with the exception of the parallel shuffled and radial shuffled distributions (p > .90). The morphed radial correlation distribution was higher than the one observed when the radial compartments were rotated (z = -23.56, p < .0001, r = -0.41, WRSt, Md = -0.04 and 0.34 respectively) but it was still not as high as that obtained in the parallel maze (z = 58.05, p < .0001, r = 0.79, WRSt, Md = 0.99 and 0.34 respectively). Inter-maze correlation distributions differed significantly (H(3,1599) = 76.3, p < .0001, Kruskal-Wallis test) and post-hoc tests confirmed that each distribution differed from every other (p < .0001 in all cases), with the exception of comparisons between compartments 1 and 4 which were both high (p > .99, Md = 0.48 and 0.45) and comparisons between compartments 2 and 3, which were both comparatively low (p > .05, Md = 0.19 and 0.20). When compared independently to shuffled distributions, all comparisons were significantly above chance (z > 12.0, p < .0001 and r > 0.40 in all cases, WRSt). When compared to the distributions obtained when rotating, correlations between compartments 1 and 4 were significantly higher when they were morphed rather than rotated (z = -16.85, p < .0001, r = -0.51, WRSt, data for 1 and 4 combined, Md = -0.03 and 0.47 respectively), and the correlations between compartments 2 and 3 remain unchanged (z = 1.48, p > .10, r = 0.03, WRSt, data for 2 and 3 combined, Md = 0.24 and 0.19 respectively) (Figure 13H).

Discussion

Many initial experiments studying place cell representations in similar environments used two compartments connected by a doorway (Tanila, 1999) or alleyway (Skaggs & McNaughton, 1998). Fuhs et al. (2005) used both configurations, so we sought to replicate their experiment in our modelled data. As reported by Fuhs et al. (2005) and Skaggs and McNaughton (1998), we found that in two parallel compartments connected by an alleyway, modelled cells often fired similarly in both compartments. Also, as reported by Fuhs et al. (2005) and Tanila (1999), we found that cells exhibited significantly more distinct representations for each compartment in two compartments connected directly by an intervening doorway.

Like Fuhs et al. (2005), we found that compartment 1 in the opposite maze configuration (top compartment in all diagrams) was represented highly similarly to both compartments in the parallel configuration. The reason for this is clear when we consider the underlying BVC inputs: since the orientation and geometry of this compartment is highly similar to the compartments in the parallel configuration, both BVC and place cell representations are nearly identical. However, in compartment 2, the shift of the doorway from the bottom to the top boundary largely disrupts activity. In their within-maze analyses, Fuhs et al. (2005) rotated compartment 2 in the opposite configuration by 180° before correlating this with compartment 1. They found that correlations between these compartments were then much lower than those between compartments in the parallel configuration. Again, our model provided the same pattern of results. However, we also found that correlations calculated without the 180° rotation were significantly higher (but still not as high as those in the parallel configuration), reflecting the maintained preferred orientation of the underlying BVCs. Whether this relationship is also true in the data of Fuhs et al. (2005) is unknown.

We modelled place cells in the four compartment apparatus used by Grieves et al. (2016b) as this allowed us to replicate both Grieves et al. (2016b) and Spiers et al.'s (2015) findings. Modelled place cells exhibited the same firing relationship and firing similarly in each of

four parallel compartments while exhibiting different representations in four radially arranged ones. The underlying process is the same as before: because local orientation and geometry in the parallel maze are highly similar for each compartment, BVC representations are nearly identical in each. However, in the radial maze, the shift in the allocentric angles and positions of the compartment walls and doorways disrupts this, resulting in divergent representations for each compartment. In support of this, when comparing the compartments between mazes, we found that correlations between compartments oriented similarly were significantly higher than between compartments at very different orientations. This result was also reported by Grieves et al. (2016b) and is easily explained using a geometric model: as the difference in orientation of the compartments increases, the change in underlying BVC representations also increases linearly.

However, this explanation suggests that the compartment rotation and correlation methods employed here and by Grieves et al. (2016b) may be inappropriate. Perhaps place cells represent compartments in the radial maze similarly, but as the compartments are rotated for correlation the place field positions are similarly rotated out of place? This would artificially reduce the similarity of compartments in the radial maze. Although it would not explain why Grieves et al. (2016b) observed significantly more place fields in the parallel maze, a result we have also replicated here. However, we sought to analyse our modelled data using an alternative 'morphing' method. Instead of rotating compartments before calculating a spatial correlation we morphed them into a new shape, thus preserving any allocentric spatial relationships. We found that this method did in fact result in higher correlations in the radial maze but these were still significantly lower than those in the parallel maze.

These results confirm that, to a certain degree, rotating compartments disrupts the underlying geometric nature of place cell firing. However, correlations in the radial maze were still lower than in the parallel maze. There are two possible reasons for this. First, as in the Fuhs et al. (2005) maze described above, the position of the doorways in the radial maze also

disrupted the firing of cells in the different compartments. Each doorway was positioned at a different angle to the centre of each box and morphing cannot rectify this disruption. This view predicts that if the orientation or indeed the shape of the compartments in the parallel maze were changed, the resulting correlations would be similar to those in the original parallel maze if they were calculated using the morphing method (as long as the doorways would still be positioned at the same angle relative to the centre of each box). Second, changing an environment's geometry without changing its size will still lead to changes in BVC activity – even if the environments are compared after morphing one to match the other. The reason for this is that each place cell receives multiple BVC inputs. As these inputs are combined, small geometric changes may lead to exaggerated changes in the place cell's activity. Thus, place cells receiving a large number of BVC inputs are likely to have seemingly unpredictable responses to environmental changes. Experiments seeking to show a predictable change in place cell firing as evidence of a geometric model of place cell firing are at risk of failure unless the precise nature of the underlying BVCs is estimated and used to model novel place cell firing as in Barry and Burgess (2007).

Overall Discussion

A minimalist, biologically tuned BVC model

We used a modified version of the boundary vector cell (BVC) model of place cell firing proposed by Hartley et al. (2000) and Barry et al. (2006) to test whether BVCs could account for place cell behaviour in environments of different size or with repetitive elements. Our model differs in a number of small, but meaningful ways. We combine BVC inputs using their geometric mean rather than their linear sum, in an attempt to produce more realistic place cell firing patterns. This approach seems to be necessary when modelling tighter, alleyway mazes, which are rarely included in BVC models of place cell activity. This is likely due to the lower

probability of BVC firing fields overlapping in an alleyway environment for summation and suggests that a multiplicative process may be more biologically plausible, despite its higher complexity. An unexpected improvement is that very well spatially modulated place cells can be generated using only two BVC inputs. We explored the effects of increased BVC inputs on place field repetition and generated place cells with a variable number of BVC inputs. However, provided that BVCs are chosen in a non-random process, whereby BVCs with similar preferred firing distances and directions are less likely to project to a single place cell, we are confident that realistic and well spatially modulated place cells can be reliably produced using very few BVC inputs. Using only two BVCs allows many place cells to be generated from fewer BVCs and requires fewer projections between the two cell populations.

In another alteration from the original models, we drew our BVC firing parameters from continuous distributions which are biased towards more biologically realistic values. In previous models, BVC preferred firing distances were drawn with equal probability from distances that increased discretely in increasing steps. This method is indirectly biased towards returning shorter distances. However, for greater control and transparency, we drew our BVC preferred firing distances from a continuous, replicable distribution that is more strongly biased towards returning short distances. The motivation for this is simply that the majority of boundary cells in the subiculum and mEC are sensitive to environmental boundaries at short distances from the animal. Nevertheless, we show that combining mainly short-distance BVCs in a multiplicative way allows for realistic place fields that can themselves be distributed far away from environmental boundaries. However, future modelling work would benefit greatly from closely matching computational parameters to real, large scale biological datasets.

The model predicts place field repetition in every case

Using this model, we generated the firing of place cells in several open field, multialleyway and multicompartment environments where place cells have been observed to

797 exhibit multiple, repeating representations. In each case, the repetition of place fields could be
798 explained almost entirely by BVC inputs to place cells, confirming that this phenomenon can be
799 driven by repeating, local geometric cues. These results further support the boundary vector cell
800 model of place cell firing. They also suggest that the firing of many place cells in the
801 hippocampus can be driven by simple, local cues and if this is the case these cells are unlikely
802 to form by themselves a global, cohesive 'cognitive map'.
803 Based on biological evidence there is good reason to believe this model is plausible; the
804 directional sensitivity of boundary cells rotate in unison with the preferred firing directions of
805 head direction (HD) cells and the grid orientation of grid cells (Perez-Escobar et al. 2016;
806 Solstad et al. 2008). When animals freely move between environments HD cells maintain the
807 same firing direction in each (Taube & Burton, 1995; Dudchenko & Zinyuk, 2005), thus we
808 would also expect boundary cells to maintain their firing relative to boundaries of a specific
809 orientation in connected environments. Indeed, in their two compartment experiment, Carpenter
810 et al. (2015) were able to record a medial entorhinal cortex boundary cell (see their
811 supplementary figure 1) which repeated the same boundary activity in the two parallel
812 compartments as predicted. This was further demonstrated in great detail by Brontons-Mas et
813 al. (2017), who inserted barriers into an open field to form four connected compartments
814 arranged in a square. Many subiculum boundary cells maintained a similar boundary sensitivity
815 in each compartment. Interestingly, not all of the boundary cells responded to the barrier inserts,
816 instead maintaining their firing relative to the original open field boundaries. In contrast, many
817 other cells were seemingly disrupted by the barriers. These interesting results demonstrate that
818 further research is needed into the characteristics and function of these underexplored cells.
819 This is apparent from recent research by Harland et al. (2017). They found that after
820 disrupting the activity of HD cells, place field repetition could be observed even in connected
821 compartments that place cells normally differentiate. It is unknown what effect disruption of the
822 HD system has on boundary cells. If they are unaffected we would need to know where they

gain their directional tuning from outside of the HD system. However, if boundary cells are affected by HD system changes, it will be important to understand how place cells compensate for this loss of input and it may suggest that BVC inputs are contextually gated, similarly to grid cells.

Grid cells and contextual gating

We have not included grid cells in the current model. Instead, we see grid cells as a means of contextual gating (Hayman, & Jeffery, 2008; Marozzi et al. 2015), allowing place cells to overcome field repetition and form distinct representations for identical environments. This view is supported by the finding that grid cells slowly develop a global representation for visually identical, connected compartments (Carpenter et al., 2015) perhaps in line temporally with learning in such environments and thus a decrease in place field repetition (Grieves et al., 2016b). This contextual input could explain why Spiers et al. (2015) observed place field remapping in one compartment of their maze upon changing its colour, despite continued repetition in the others. Geometry and thus BVC inputs remained the same, but a contextual change caused remapping in both grid and place cells only in that compartment. We would also suggest that, as with other environmental cues, some place cells are likely driven more strongly by geometric or contextual inputs, thus place field repetition may not be exhibited by all place cells to the same extent. This also explains why spatial correlation values found in multicompartment experiments form a distribution, centred on a high value but spread across a range of values (Grieves et al., 2016b; Skaggs & McNaughton, 1998; Spiers et al., 2015).

In summary, we present a purely geometric model of place cell firing which we have used to replicate the activity of these cells in a number of published experiments. Together with the behavioural and recording evidence indicating that the shape of the environment guides spatial learning (e.g., Cheng, 1986; Gallistel, 1990; Hermer & Spelke, 1994; Learnmonth et al.,

2002; Hupbach & Nadel, 2005; Julian et al., 2015; Keinath et al., 2017; Weis et al., 2017), this model suggests that geometry exerts a strong influence on spatial cognition. Our results show that the field repetition activity of place cells observed in environments with similar or repetitive geometric components, can largely be accounted for by boundary vector cell inputs.

Acknowledgements

We would like to thank Professor Neil Burgess for suggesting a BVC model approach to investigating place field repetition and for his subsequent help and advice in understanding the original model and its parameters. We would also like to thank Dr. Colin Lever for insights into the specific characteristics of boundary vector cells in the brain.

References

Alme, C. B., Miao, C., Jezek, K., Treves, A., Moser, E. I. & Moser, M-B. (2014) Place cells in the hippocampus: Eleven maps for eleven rooms. *PNAS*, 111(52), 18428–18435

Anderson, M. I., & Jeffery, K. J. (2003). Heterogeneous modulation of place cell firing by changes in context. *The Journal of Neuroscience: The Official Journal of the Society for Neuroscience*, *23*(26), 8827–8835.

Barry, C., & Burgess, N. (2007). Learning in a geometric model of place cell firing. *Hippocampus*, *17*(9), 786–800.

Barry, C., Lever, C., Hayman, R., Hartley, T., Burton, S., O'Keefe, J., Burgess, N. (2006). The boundary vector cell model of place cell firing and spatial memory. *Reviews in the Neurosciences*, *17*(1-2), 71–97.

Bjerknes, T. L., Moser, E. I., & Moser, M.-B. (2014). Representation of geometric borders in the developing rat. *Neuron*, *82*(1), 71–78.

Boccara, C. N., Sargolini, F., Thoresen, V. H., Solstad, T., Witter, M. P., Moser, E. I., & Moser, M.-B. (2010). Grid cells in pre- and parasubiculum. *Nature Neuroscience*, *13*(8), 987–994.

Bostock, E., Muller, R. U. & Kubie, J. L. (1991). Experience-dependent modifications of hippocampal place cell firing. *Hippocampus*. 1(2), 193-205

Brontons-Mas, J. R., Schaffelhofer, S., Guger, C., O'Mara, S. M. & Sanchez-Vives, M. V. (2017) Heterogeneous spatial representation by different subpopulations of neurons in the subiculum. *Neuroscience*. 343, 174-189

Burgess, N., Donnett, J. G., Jeffery, K. J., & O-keefe, J. (1997). Robotic and neuronal simulation of the hippocampus and rat navigation. *Philosophical Transactions of the Royal Society of London. Series B, Biological Sciences*, *352*(1360), 1535–1543.

Burgess, N., Jackson, A., Hartley, T., & O'Keefe, J. (2000). Predictions derived from modelling the hippocampal role in navigation. *Biological Cybernetics*, *83*(3), 301–312.

Bush, D., Barry, C., & Burgess, N. (2014). What do grid cells contribute to place cell firing? *Trends in Neurosciences*, *37*(3), 136–145.

Carpenter, F., Manson, D., Jeffery, K., Burgess, N., & Barry, C. (2015). Grid cells form a global representation of connected environments. *Current Biology: CB*, *25*(9), 1176–1182.

Cowen, S. L., & Nitz, D. A. (2014). Repeating firing fields of CA1 neurons shift forward in response to increasing angular velocity. *The Journal of Neuroscience: The Official Journal of the Society for Neuroscience*, *34*(1), 232–241.

Derdikman, D., Whitlock, J. R., Tsao, A., Fyhn, M., Hafting, T., Moser, M.-B., & Moser, E. I. (2009). Fragmentation of grid cell maps in a multicompartment environment. *Nature Neuroscience*, *12*(10), 1325–1332.

Dudchenko, P. A. & Zinyuk, L. E. (2005). The formation of cognitive maps of adjacent environments: Evidence from the head direction cell system. *Behavioral Neuroscience*. *119*(6), 1511-1523

Eichenbaum, H., Howard, E., Paul, D., Emma, W., Matthew, S., & Heikki, T. (1999). The Hippocampus, Memory, and Place Cells. *Neuron*, *23*(2), 209–226.

Frank, L. M., Brown, E. N., & Wilson, M. (2000). Trajectory encoding in the hippocampus and entorhinal cortex. *Neuron*, *27*(1), 169–178.

Fuhs, M. C., Vanrhoads, S. R., Casale, A. E., McNaughton, B., & Touretzky, D. S. (2005). Influence of path integration versus environmental orientation on place cell remapping between visually identical environments. *Journal of Neurophysiology*, *94*(4), 2603–2616.

Gallistel, C.R. (1990). *The Organisation of Learning*. Bradford Books/MIT Press.

Girardeau, G., Benchenane, K., Wiener, S. I., Buzsáki, G., Zugaro, M. B. (2009) Selective suppression of hippocampal ripples impairs spatial memory. *Nat Neurosci*, 12(10):1222-3.

Grieves, R. M. (2015, January 26). *The Neural Basis of a Cognitive Map*. University of Stirling. Retrieved from http://hdl.handle.net/1893/21878

Grieves, R. M., Wood, E. R. & Dudchenko, P. A. (2016a). Place cells on a maze encode routes

rather than destinations. *eLife*, 5:e15986. DOI: 10.7554/eLife.15986

Grieves, R. M., Jenkins, B. W., Harland, B. C., Wood, E. R., & Dudchenko, P. A. (2016b). Place field repetition and spatial learning in a multicompartment environment. *Hippocampus*, *26*(1), 118–134.

Grieves R. M., Duvelle É, Wood E. R. & Dudchenko, P. A. (2017b) Field repetition and local mapping in the hippocampus and medial entorhinal cortex, *Journal of Neurophysiology* (Forthcoming/Available Online)

Harland, B., Grieves, R. M., Bett, D., Stentiford, R., Wood, E. R. & Dudchenko, P. A. (2017) Lesions of the Head Direction Cell System Increase Hippocampal Place Field Repetition, *Current Biology*, 27(17), 2706-2712.

Hartley, T., Burgess, N., Lever, C., Cacucci, F., & O'Keefe, J. (2000a). Modeling place fields in terms of the cortical inputs to the hippocampus. *Hippocampus*, *10*(4), 369–379.

Hayman, R. M., & Jeffery, K. J. (2008). How heterogeneous place cell responding arises from homogeneous grids--a contextual gating hypothesis. *Hippocampus*, *18*(12), 1301–1313.

Hermer, L., & Spelke, E.S. (1994). A geometric process for spatial reorientation in young children. *Nature, 370:* 57-59.

Hupbach, A., Nadel, L. (2005). Reorientation in a rhombic environment: no evidence for an encapsulated geometric module. *Cognitive Development*, *20,* 279-302.

Jankowski, M. M., & O'Mara, S. M. (2015). Dynamics of place, boundary and object encoding in rat anterior claustrum. *Frontiers in Behavioral Neuroscience*, *9*, 250.

Jankowski, M. M., Passecker, J., Islam, M. N., Vann, S., Erichsen, J. T., Aggleton, J. P., & O'Mara, S. M. (2015). Evidence for spatially-responsive neurons in the rostral thalamus. *Frontiers in Behavioral Neuroscience*, *9*, 256.

Julian, J.B., Keinath, A.T., Muzzio, I.A., & Epstein, R.A. (2015). Place recognition and heading retrieval are mediated by dissociable cognitive systems in mice. *Proceedings of the National Academy of Sciences*, *112(20)*, 6503-6508.

Keinath, A.T., Julian, J.B., Epstein, R.A., & Muzzio, I.A. (2017). Environmental geometry aligns the hippocampal map during spatial reorientation. *Current Biology*, *27,* 309-317

Kentros, C. G., Agnihotri, N. T., Streater, S., Hawkins, R. D. & Kandel, E. R. (2004) Increased Attention to Spatial Context Increases Both Place Field Stability and Spatial Memory. *Neuron*, 42(2), 283-295

Langston, R. F., Ainge, J. A., Couey, J. J., Canto, C. B., Bjerknes, T. L., Witter, M. P., … Moser, M.-B. (2010). Development of the spatial representation system in the rat. *Science*, *328*(5985), 1576–1580.

Learmonth, A.E., Nadel, L., & Newcombe, N.S. (2002). Children's use of landmarks: implications for modularity theory. *Psychological Science*, *13,* 337-341.

Leutgeb, S., Leutgeb, J. K., Barnes, C. A., Moser, E. I., McNaughton, B. L., & Moser, M.-B. (2005). Independent codes for spatial and episodic memory in hippocampal neuronal ensembles. *Science*, *309*(5734), 619–623.

Lever, C., Burgess, N., Cacucci, F., Hartley, T., & O'Keefe, J. (2002). What can the hippocampal representation of environmental geometry tell us about Hebbian learning? *Biological Cybernetics*, *87*(5-6), 356–372.

Lever, C., Burton, S., Jeewajee, A., O'Keefe, J., & Burgess, N. (2009). Boundary vector cells in the subiculum of the hippocampal formation. *The Journal of Neuroscience: The Official Journal of the Society for Neuroscience*, *29*(31), 9771–9777.

Lever C, Cacucci F, Burgess N, O'Keefe J. (1999). Squaring the circle: place cell firing patterns in environments which differ only geometrically are not unpredicatable. In *Society for Neuroscience Abstract* (p. 24:556).

Lever, C., Wills, T., Cacucci, F., Burgess, N., & O'Keefe, J. (2002). Long-term plasticity in hippocampal place-cell representation of environmental geometry. *Nature*, *416*(6876), 90–94.

Marozzi, E., Ginzberg, L. L., Alenda, A., & Jeffery, K. J. (2015). Purely Translational

Realignment in Grid Cell Firing Patterns Following Nonmetric Context Change. Cerebral Cortex (New York, NY), 25(11), 4619–4627. http://doi.org/10.1093/cercor/bhv120

McNaughton, B. L., Barnes, C. A., & O'Keefe, J. (1983). The contributions of position, direction, and velocity to single unit activity in the hippocampus of freely-moving rats. *Experimental Brain Research. Experimentelle Hirnforschung. Experimentation Cerebrale*, *52*(1), 41–49.

Morris, R. G. M. (1981). Spatial localization does not require the presence of local cues. *Learning and Motivation*, *12*(2), 239–260.

Muessig, L., Hauser, J., Cacucci, F. (2016) Place Cell Networks in Pre-weanling Rats Show Associative Memory Properties from the Onset of Exploratory Behavior. *Cerebral Cortex*. 26(8), 3627–3636

Muessig, L., Hauser, J., Wills, J. T., Cacucci, F. (2015) A Developmental Switch in Place Cell Accuracy Coincides with Grid Cell Maturation. *Neuron*. 86, 1167–1173

Muller, R. U., & Kubie, J. L. (1987). The effects of changes in the environment on the spatial firing of hippocampal complex-spike cells. *The Journal of Neuroscience: The Official Journal of the Society for Neuroscience*, *7*(7), 1951–1968.

Muller, R. U., Kubie, J. L., & Ranck, J. B., Jr. (1987). Spatial firing patterns of hippocampal complex-spike cells in a fixed environment. *The Journal of Neuroscience: The Official Journal of the Society for Neuroscience*, *7*(7), 1935–1950.

Navratilova, Z., Hoang, L. T., Schwindel, C. D., Tatsuno, M., & McNaughton, B. L. (2012). Experience-dependent firing rate remapping generates directional selectivity in hippocampal place cells. *Frontiers in Neural Circuits*, *6*, 6.

Nitz, D. A. (2011). Path shape impacts the extent of CA1 pattern recurrence both within and across environments. *Journal of Neurophysiology*, *105*(4), 1815–1824.

O'Keefe, J. (1979). A review of the hippocampal place cells. *Progress in Neurobiology*, *13*(4), 419–439.

O'Keefe, J., & Burgess, N. (1996). Geometric determinants of the place fields of hippocampal

neurons. *Nature*, *381*(6581), 425–428.

O'Keefe, J., & Conway, D. H. (1978). Hippocampal place units in the freely moving rat: why they fire where they fire. *Experimental Brain Research. Experimentelle Hirnforschung. Experimentation Cerebrale*, *31*(4), 573–590.

O'Keefe, J. (1976). Place units in the hippocampus of the freely moving rat. *Experimental Neurology*, *51*(1), 78–109.

O'Keefe, J., & Nadel, L. (1978). *The hippocampus as a cognitive map*. Oxford University Press, USA.

Paz-Villagrán, V., Save, E., & Poucet, B. (2004). Independent coding of connected environments by place cells. *The European Journal of Neuroscience*, *20*(5), 1379–1390.

Peña, J. L., & Konishi, M. (2001). Auditory spatial receptive fields created by multiplication. *Science*, *292*(5515), 249–252.

Pérez-Escobar, J. A., Kornienko, O., Latuske, P., Kohler, L. & Allen, K. (2016) Visual landmarks sharpen grid cell metric and confer context specificity to neurons of the medial entorhinal cortex. *eLife*. eLife 2016;5:e16937

Peña, J. L., & Konishi, M. (2004). Robustness of multiplicative processes in auditory spatial tuning. *The Journal of Neuroscience: The Official Journal of the Society for Neuroscience*, *24*(40), 8907–8910.

Pfeiffer, E. & Foster, D. J. (2013) Hippocampal place-cell sequences depict future paths to remembered goals. *Nature*, 497, 74–79

Raudies, F., & Hasselmo, M. E. (2012). Modeling boundary vector cell firing given optic flow as a cue. *PLoS Computational Biology*, *8*(6), e1002553.

Savelli, F., Yoganarasimha, D., & Knierim, J. J. (2008). Influence of boundary removal on the spatial representations of the medial entorhinal cortex. *Hippocampus*, *18*(12), 1270–1282.

Schnupp, J. W., & King, A. J. (2001). Neural processing: the logic of multiplication in single neurons. *Current Biology: CB*, *11*(16), R640–2.

Sharp, P. E. (1997). Subicular cells generate similar spatial firing patterns in two geometrically and visually distinctive environments: comparison with hippocampal place cells. *Behavioural Brain Research*, *85*(1), 71–92.

Sharp, P. E. (1999). Subicular place cells expand or contract their spatial firing pattern to fit the size of the environment in an open field but not in the presence of barriers: comparison with hippocampal place cells. *Behavioral Neuroscience*, *113*(4), 643–662.

Singer, A. C., Karlsson, M. P., Nathe, A. R., Carr, M. F., & Frank, L. M. (2010). Experience-dependent development of coordinated hippocampal spatial activity representing the similarity of related locations. *The Journal of Neuroscience: The Official Journal of the Society for Neuroscience*, *30*(35), 11586–11604.

Skaggs, W. E., & McNaughton, B. L. (1998). Spatial firing properties of hippocampal CA1 populations in an environment containing two visually identical regions. *The Journal of Neuroscience: The Official Journal of the Society for Neuroscience*, *18*(20), 8455–8466.

Solstad, T., Boccara, C. N., Kropff, E., Moser, M.-B., & Moser, E. I. (2008). Representation of Geometric Borders in the Entorhinal Cortex. *Science*, *322*(5909), 1865–1868.

Spiers, H. J., Hayman, R. M. A., Jovalekic, A., Marozzi, E., & Jeffery, K. J. (2015). Place field repetition and purely local remapping in a multicompartment environment. *Cerebral Cortex* , *25*(1), 10–25.

Stewart, S., Jeewajee, A., Wills, T. J., Burgess, N., & Lever, C. (2014). Boundary coding in the rat subiculum. *Philosophical Transactions of the Royal Society of London. Series B, Biological Sciences*, *369*(1635), 20120514.

Tanila, H. (1999). Hippocampal place cells can develop distinct representations of two visually identical environments. *Hippocampus*, *9*(3), 235–246.

Taube, J. S., Burton, H. L. (1995) Head direction cell activity monitored in a novel environment and during a cue conflict situation. *Journal of Neurophysiology*, *74*(5), 1953-1971

Thompson, L. T., & Best, P. J. (1989). Place cells and silent cells in the hippocampus of freely-

behaving rats. *The Journal of Neuroscience: The Official Journal of the Society for Neuroscience*, *9*(7), 2382–2390.

Weiss, S., Talhami, G., Gofman-Regev, X., Rapoport, S., Eilam, D., Derdikman, D. (2017). Consistency of spatial representations in rat entorhinal cortex predicts performance in a reorientation task. *Current Biology, 27*, 3658-3665.

Thompson, L. T., & Best, P. J. (1990). Long-term stability of the place-field activity of single units recorded from the dorsal hippocampus of freely behaving rats. *Brain Research*, *509*(2), 299–308.

Wills, T. J., Barry, C., & Cacucci, F. (2012). The abrupt development of adult-like grid cell firing in the medial entorhinal cortex. *Frontiers in Neural Circuits*, *6*. https://doi.org/10.3389/fncir.2012.00021

Wilson, M. A., & McNaughton, B. L. (1993). Dynamics of the hippocampal ensemble code for space. *Science*, *261*(5124), 1055–1058.

Yoganarasimha, D., & Knierim, J. J. (2005). Coupling between place cells and head direction cells during relative translations and rotations of distal landmarks. *Experimental Brain Research. Experimentelle Hirnforschung. Experimentation Cerebrale*, *160*(3), 344–359.